STEM CELLS AND REGENERATION

RESEARCH ARTICLE

The E2A splice variant E47 regulates the differentiation of projection neurons via p57(KIP2) during cortical development

Sabrina Pfurr[1,2,‡], Yu-Hsuan Chu[1,2,‡], Christian Bohrer[1,2], Franziska Greulich[3], Robert Beattie[4,*], Könül Mammadzada[1,2], Miriam Hils[2,5], Sebastian J. Arnold[6,7], Verdon Taylor[4], Kristina Schachtrup[2,5], N. Henriette Uhlenhaut[3] and Christian Schachtrup[1,§]

ABSTRACT

During corticogenesis, distinct classes of neurons are born from progenitor cells located in the ventricular and subventricular zones, from where they migrate towards the pial surface to assemble into highly organized layer-specific circuits. However, the precise and coordinated transcriptional network activity defining neuronal identity is still not understood. Here, we show that genetic depletion of the basic helix-loop-helix (bHLH) transcription factor E2A splice variant E47 increased the number of Tbr1-positive deep layer and Satb2-positive upper layer neurons at E14.5, while depletion of the alternatively spliced E12 variant did not affect layer-specific neurogenesis. While ChIP-Seq identified a big overlap for E12- and E47-specific binding sites in embryonic NSCs, including sites at the cyclin-dependent kinase inhibitor (CDKI) *Cdkn1c* gene locus, RNA-Seq revealed a unique transcriptional regulation by each splice variant. E47 activated the expression of the CDKI *Cdkn1c* through binding to a distal enhancer. Finally, overexpression of E47 in embryonic NSCs *in vitro* impaired neurite outgrowth, and overexpression of E47 *in vivo* by *in utero* electroporation disturbed proper layer-specific neurogenesis and upregulated p57(KIP2) expression. Overall, this study identifies E2A target genes in embryonic NSCs and demonstrates that E47 regulates neuronal differentiation via p57(KIP2).

INTRODUCTION

The mammalian cerebral cortex is a complex six-layered structure whose cellular composition and organization underlies our highest cognitive, perceptual and motor functions. During cortical development, multipotent embryonic neural stem cells (NSCs), also referred to as radial glia (RG) cells, span the width of the brain wall, retaining their cell bodies in the ventricular zone (VZ) (Pinto and Gotz, 2007). RG cells undergo neurogenic asymmetric divisions to generate a proliferating RG and a more differentiated cell, either a neuron or a basal intermediate progenitor (IP). Immature neurons migrate out of the VZ where they become functionally integrated mature neurons and contribute to outer layer formation, while IPs migrate into the subventricular zone (SVZ) and proliferate to amplify the neurogenic population. RG and IP cells give rise to six cortical layers in an 'inside out' order, from the deepest layer VI, which contains early-born neurons, to layer II, which is populated by the latest born neurons (Molyneaux et al., 2007). During brain development, specification of neuronal identity is orchestrated by the sequential expression of genes that control proliferation, cellular migration and neuronal differentiation (Kwan et al., 2012; Molyneaux et al., 2015; Telley et al., 2016).

Basic helix-loop-helix (bHLH) transcription factors (TFs) play key roles in self-renewal and fate determination of NSCs during corticogenesis (Imayoshi and Kageyama, 2014; Lee, 1997; Ross et al., 2003; Vetter, 2001). bHLH TFs are characterized by a highly conserved helix-loop-helix domain comprising two amphipathic α-helices separated by a loop of variable length, which mediates the formation of homo- or heterodimers (Murre et al., 1994). This family of TFs contains a second motif of mainly basic amino acid residues that allows DNA binding to a consensus hexanucleotide E box sequence (CANNTG) (Murre et al., 1994; Voronova and Baltimore, 1990). Class I bHLH TFs, called E proteins, have the ability to function as heterodimers with class II bHLH proteins, including members of the achaete-scute [e.g. Mash1 (Ascl1)], neurogenin (Ngn1 and Ngn2) and NeuroD families (e.g. NeuroD1), for controlling differentiation and specification of NSCs and IPs during embryonic development (Lee, 1997; Wang and Baker, 2015).

E proteins are encoded by three genes, namely *Tcf3* (E2A), *Tcf4* (E2-2) and *Tcf12* (HEB). The *Tcf3* gene codes for the alternative splice variants E12 and E47. Beside its heterodimer activity with proneural TFs, E2A can interact with TFs from the Ets and Pax families and, particularly E47, has been demonstrated to act as a homodimer during B cell development (Shen and Kadesch, 1995). E2A target genes during cortical development are unknown; however, it has been demonstrated that it regulates cell cycle progression through activation of cyclin-dependent kinase inhibitors (CDKI), and cadherin-mediated cell adhesion through transcriptional repression of E-cadherin (Pagliuca et al., 2000; Pérez-Moreno et al., 2001; Prabhu et al., 1997; Rothschild et al., 2006). Differential E protein expression patterns during brain development and exclusive E2A expression in adult NSCs of the SVZ stem cell niche suggests that E proteins act during orchestration

[1]Institute of Anatomy and Cell Biology, Faculty of Medicine, University of Freiburg, Freiburg 79104, Germany. [2]Faculty of Biology, University of Freiburg, Freiburg 79104, Germany. [3]Helmholtz Diabetes Center (HDC) and German Center for Diabetes Research (DZD), Helmholtz Zentrum München, Neuherberg 85764, Germany. [4]Department of Biomedicine, Embryology and Stem Cell Biology, University of Basel, Basel 4058, Switzerland. [5]Center for Chronic Immunodeficiency (CCI), Medical Center – University of Freiburg, Faculty of Medicine, University of Freiburg, Freiburg 79106, Germany. [6]Institute of Experimental and Clinical Pharmacology and Toxicology, Faculty of Medicine, University of Freiburg, Freiburg 79104, Germany. [7]BIOSS Centre of Biological Signalling Studies, Albert-Ludwigs-University, Freiburg 79104, Germany.
*Present address: Developmental Neurobiology, IST Austria (Institute of Science and Technology Austria), Klosterneuburg 3400, Austria.
‡These authors contributed equally to this work

§Author for correspondence (christian.schachtrup@anat.uni-freiburg.de)

C.S., 0000-0001-9851-6299

DEVELOPMENT

of early cortical developmental processes (Bohrer et al., 2015; Ravanpay and Olson, 2008; Roberts et al., 1993). Initial generation and characterization of the E2A splice variant E12 and E47 knockout mice revealed that these splice variants fulfill distinct functions in B cell lineage specification (Beck et al., 2009). However, the precise contributions of these E2A splice variants and their target genes to cortical neurogenesis and specification of neural subtype identities is not known.

Here, we have identified the CDKI gene *Cdkn1c* as a functional target of E2A during neurogenesis. E47-deficient mouse embryos had an increase in the number of cortical plate neurons at E14.5, despite equal cell cycle progression of NSCs. Overexpression of E47 in embryonic NSCs led to upregulation of *Cdkn1c* mRNA and inhibition of neuronal differentiation. Upon E47 overexpression *in vivo* by *in utero* electroporation, p57 (KIP2) protein abundance was increased in cortical precursor cells and neuronal localization as well as neurite outgrowth was impaired. Our results suggest that the E2A splice variant E47 controls neurogenesis via the CDKI p57(KIP2) as an E47-regulated key factor in neuronal specification.

RESULTS

The E2A splice variants E12 and E47 exhibit comparable spatiotemporal expression patterns during cortical development

To investigate the role of the E2A splice variants E12 and E47 in embryonic NSCs during cortical development (Fig. 1A), we first examined the temporal expression of E2A around the peak of cortical neurogenesis. *In situ* RNA hybridization analysis showed *Tcf3* expression in cells located in the VZ and SVZ of the cortex at embryonic day 14.5 (E14.5) (Fig. S1A), consistent with expression by mitotic embryonic NSCs and progenitors. Quantitative PCR for the E2A splice variants E12 and E47 on FACS-sorted NSCs (Hes5:: eGFP sorted NSCs) of different developmental stages (E11.5, E15.5 and E18.5) showed highest expression of both splice variants at E15.5 (Fig. 1B). Immunolabeling for E2A protein at E14.5 showed variegated E2A expression levels in distinct cell populations in the developing cortex (Fig. 1C). E2A was expressed by Pax6$^+$ cells, separating this cell population into either high or low E2A-expressing progenitors, with higher E2A expression in Pax6$^+$ cells in the apical region of the VZ (Fig. 1D). Most *Eomes*$^{GFP+}$ (Eomes,
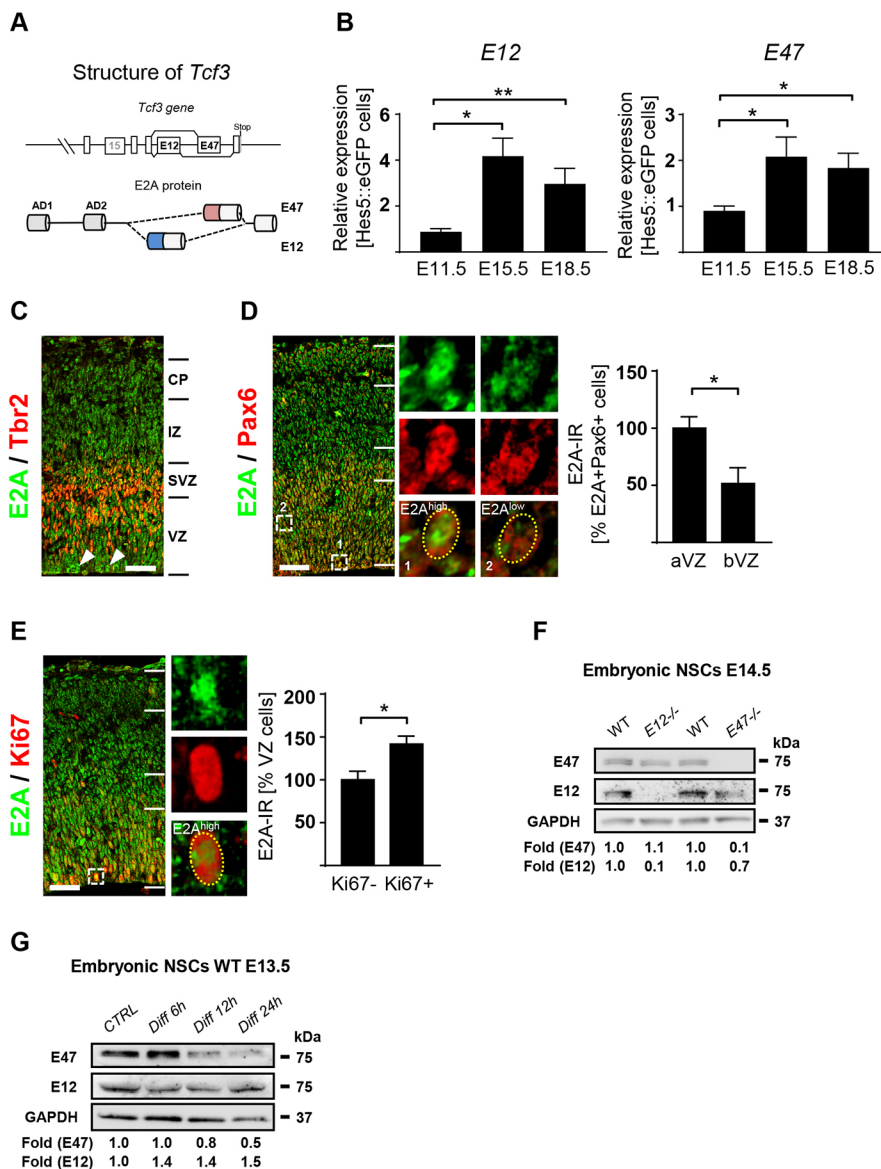

Fig. 1. Expression of the E2A splice variants E12 and E47 in the developing cortex. (A) Structure of the *Tcf3* locus. The alternatively spliced E12 and E47 proteins differ only in their DNA-binding region. (B) Expression of the E2A splice variants E12 and E47 in FACS-isolated neural stem cells at embryonic days 11.5, 15.5 and 18.5 in HES5::eGFP mice. Results are from at least three independent experiments performed in duplicate. (C) Immunolabeling for E2A (green) and Tbr2 (red) in the cortex in representative sagittal brain sections of C57BL/6 mice at E14.5. Arrowheads depict high E2A-expressing cells in the VZ. Scale bar: 45 μm. (*n*=3). (D,E) Immunolabeling for E2A (green) in combination with Pax6 (D, red) or Ki67 (E, red) in sagittal brain sections of mice at E14.5. White boxes indicate representative E2A colocalization with Pax6$^+$ (D) and Ki67$^+$ (E) cells (high magnification images are on the right). The graphs show quantification of E2A immunoreactivity per total E2A$^+$Pax6$^+$ cells in the apical and basal VZ (D, right) or in E2A$^+$Ki67$^+$ cells in the VZ (E, right). Scale bars: 45 μm. (*n*=3). (F) Immunoblot protein expression analysis for E47 and E12 in embryonic wild-type, E12$^{-/-}$ and E47$^{-/-}$ NSCs cultured under proliferation conditions. Representative western blots are shown from two (E12) and three (E47) independent experiments. (G) Immunoblot protein expression analysis for E47 and E12 in embryonic wild-type NSCs cultured under proliferation and differentiation conditions. Representative western blots are shown from six independent experiments. **P<0.01, *P<0.05 by one-way ANOVA (B) and Student's *t*-test (D,E). CP, cortical plate; IZ, intermediate zone; SVZ, subventricular zone; VZ, ventricular zone; aVZ, apical region of VZ; bVZ, basal region of VZ.

DEVELOPMENT

also referred to as Tbr2) IPs and Tuj-1$^+$ immature neurons showed a moderate level of E2A expression (Fig. S1B,C), suggesting that E2A levels might decrease in differentiating cells. Accordingly, high E2A expression coincided with proliferating Ki67$^+$ cells in the VZ (Fig. 1E), indicating a role for E2A in embryonic NSC maintenance and differentiation. In addition, high E2A expression was also observed in some cells of the upper layer of the cortical plate (Fig. S1B,C). To elucidate the specific protein abundance of the E2A splice variants E12 and E47, we first performed western blotting on E12$^{-/-}$ and E47$^{-/-}$ NSCs to confirm antibody specificity (Fig. 1F). The E12 protein abundance increased, while the E47 protein abundance decreased during the temporal progress of embryonic NSC differentiation (Fig. 1G), suggesting that both splice variants might differently regulate neuronal differentiation of precursor cells in the VZ and SVZ.

E47 deficiency leads to increased numbers of Tbr1$^+$ and Satb2$^+$ neurons, while E12 has no effect on cortical neurogenesis

To study the functions of the E2A splice variants E12 and E47 in the developing cortex, we examined the impact of splice variant-

specific loss of function on the specification of NSCs and their progeny. Detailed cortical layer analysis at E14.5 revealed a significant increase in the total number of Tbr1$^+$ [layer VI; E47$^{-/-}$, 1.52±0.18-fold (±s.e.m.); $P<0.05$: Fig. 2A,C] and Satb2$^+$ [layer II-V; E47$^{-/-}$, 1.6±0.06-fold (±s.e.m.); $P<0.01$: Fig. 2B,D] neurons in E47$^{-/-}$ embryos compared with wild-type embryos. The number of Tbr1$^+$ neurons was also significantly, albeit not as drastically, increased at E18.5; at postnatal day 3 (P3) there was no significant difference in the number of Tbr1$^+$ cells in E47$^{-/-}$ embryos compared with wild-type embryos (Fig. S2A-D), while the total number of Satb2$^+$ early-born neurons was similar at E18.5 and P3 in E47$^{-/-}$ embryos compared with wild-type embryos (Fig. S2E,F and data not shown). E12$^{-/-}$ embryos showed no difference in Tbr1$^+$ and Satb2$^+$ cells compared with littermate controls at E14.5 (Fig. S2G-J), suggesting that specifically E47 controls neuronal identities. Bin analysis showed an equal increase in the number of Tbr1$^+$ neurons located in bins 1 to 5 in E47$^{-/-}$ embryos compared with control (Fig. 2E), illustrating that the increase in Tbr1$^+$ cells in E47$^{-/-}$ animals is not due to a shift in the localization of early-born neurons. Interestingly, Ctip2$^+$ cells, which represent subcortical projection neurons of layer V, were not affected in E47$^{-/-}$ embryos
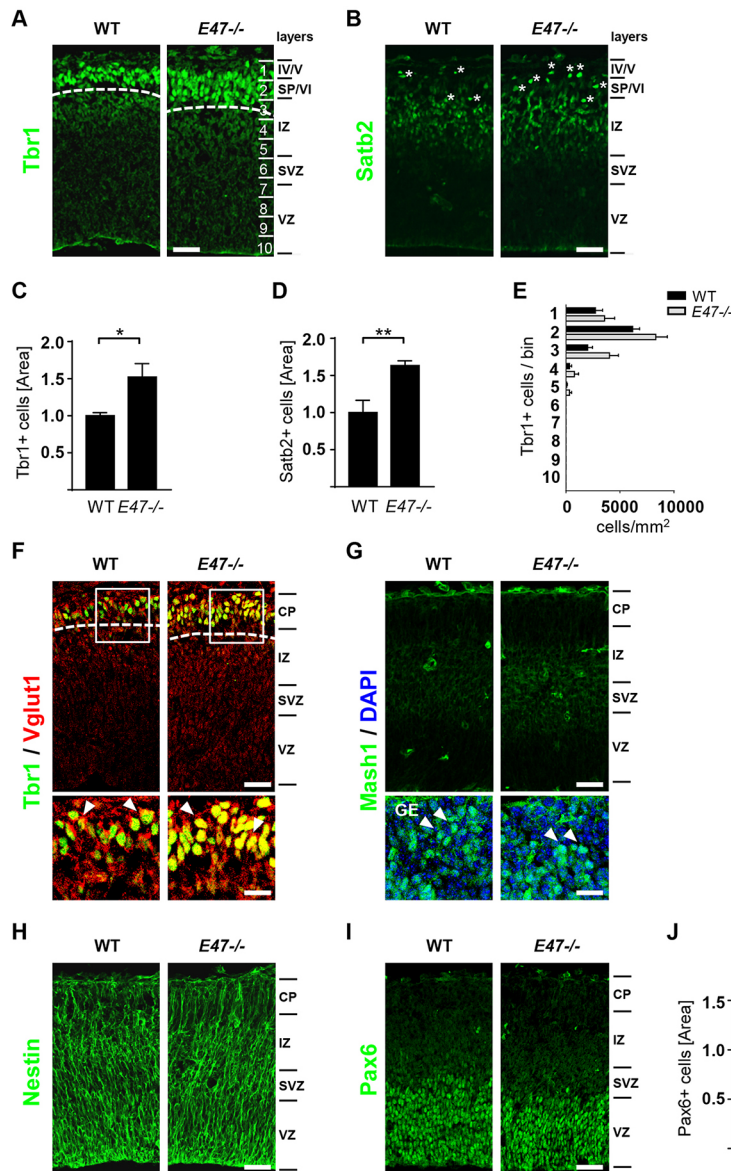

Fig. 2. E47 regulates Tbr1$^+$ and Satb2$^+$ neurogenesis at E14.5. (A,B) Immunolabeling for Tbr1 (A, green) and Satb2 (B, green) in sagittal brain sections of E47$^{-/-}$ mice compared with wild-type littermates at E14.5. The radial extent of the cortical wall was divided into 10 bins of equivalent height. Scale bars: 40 μm. (C,D) Quantification of the number of Tbr1$^+$ (C) and Satb2$^+$ (D) neurons ($n=5$ wild-type mice, $n=4$ E47$^{-/-}$ mice, C; $n=5$ wild-type mice, $n=6$ E47$^{-/-}$ mice, D). (E) Quantification of Tbr1$^+$ cells located in each of 10 bins throughout the cortex in sagittal sections of E47$^{-/-}$ mice and wild-type littermates at E14.5 ($n=4$ mice). (F,G) Immunolabeling for Vglut1 (red) in combination with Tbr1 (green) (F), or immunolabeling for Mash1 (green) (G) in representative sagittal brain sections of E47$^{-/-}$ mice compared with wild-type littermates at E14.5. Nuclei are stained with DAPI (blue). Scale bars: 40 μm, top; 17 μm, bottom. $n=3$ mice. (H) Immunolabeling for nestin (green) in the cortex in representative sagittal sections of E47$^{-/-}$ mice compared with wild-type littermates at E14.5. Scale bar: 40 μm. $n=4$ mice. (I) Immunolabeling for Pax6 (green) in sagittal sections of E47$^{-/-}$ mice compared with wild-type littermates at E14.5. Scale bar: 40 μm. (J) Quantification of the number of Pax6$^+$ radial glial cells in cortical brain sections of E47$^{-/-}$ mice and wild-type littermates at E14.5 ($n=4$ wild-type mice, $n=3$ E47$^{-/-}$ mice). Data are mean±s.e.m. **$P<0.01$; *$P<0.05$ using Student's t-test. CP, cortical plate; GE, ganglionic eminence; IV/V, cortical layer IV/V; IZ, intermediate zone; SP, subplate; SVZ, subventricular zone; VI, cortical layer VI; VZ, ventricular zone.

compared with wild-type littermates, suggesting that E47 regulates neurogenesis of distinct populations of excitatory cortical neurons (Fig. S2K,L). bHLH TF Ngn1 and Ngn2 have been shown to specify the properties of early-born neurons and *Ngn* mutants reveal a global shift of neuronal phenotype from cortical, glutamatergic to subcortical, GABAergic neurons (Schuurmans et al., 2004). As E47 has the ability to function as heterodimer with class II bHLH proteins, including Ngn1 and Ngn2, we analyzed whether E47 depletion results in identity changes of Tbr1^{+} neocortical neurons. Immunolabeling for Vglut1, a marker for glutamatergic neurons, and Math2, a TF expressed by cortical neurons, revealed that the population of Tbr1^{+} cells in E47^{−/−} mice had not changed its identity (Fig. 2F and data not shown). Mash1 protein levels were strongly upregulated in *Ngn2* mutants (Schuurmans et al., 2004). In contrast, Mash1 expression was almost absent in the cortex and was not further upregulated in E47^{−/−} brain sections (Fig. 2G). Tbr1^{+} neurons are the source of neurofilament[+] corticothalamic axons (Bedogni et al., 2010) and, in accordance with no identity change of Tbr1^{+} neurons in E47^{−/−} mice, they appeared with normal shape (Fig. S2M,N). E2A splice variants are thought to be an essential heterodimerization partner of the proneural bHLH TFs Mash1 and Ngn2 to facilitate DNA binding. *Ngn2;Mash1* double-mutant embryos have a severe disruption of the cortical cytoarchitecture (Nieto et al., 2001). However, neither E47^{−/−} nor E12^{−/−} embryos had any overt differences in RG cell organization and cortex cytoarchitecture compared with wild type, as shown by immunolabeling for nestin (Fig. 2H; Fig. S2O). Furthermore, quantification of Pax6^{+} or Sox2^{+} RG cells in E47^{−/−} embryos and Pax6^{+} RG cells in E12^{−/−} embryos revealed no significant differences compared with wild-type controls (Fig. 2I,J; Fig. S2P-S). Loss of E47 did not significantly alter the Tbr2^{+} and Ngn2^{+} IPs and neurogenic cell population, respectively, nor did it affect the differentiation of NeuN^{+} neurons or apoptosis at E14.5 (Fig. S3) and E18.5 (data not shown, cleaved caspase 3). Overall, these results reveal that E47 controls the number of Tbr1^{+} and Satb2^{+} neurons at E14.5.

E2A binds to a variety of genes controlling cortical brain development

To identify E2A target genes during cerebral cortex development, we performed genome-wide mapping of E2A-bound sequences in primary NSCs using chromatin immunoprecipitation combined with DNA sequencing (ChIP-Seq). As splice variant-specific antibodies are not suitable for ChIP experiments due to their selective detection of DNA-bound regions, we used an antibody that recognizes both E12 and E47, and chromatin prepared from the mouse dorsal telencephalon at E12.5 (Fig. 3A), a stage when most cells in the cortex are progenitors and where E2A protein was highly abundant. Motif analysis of *cis*-regulatory sequences associated with E2A protein occupancy revealed that the E protein consensus DNA sequence (CAGCTG; E-box) was ranked as the top-scoring motif (Fig. 3B). E2A-bound regions were enriched for Sox family member and E2f6-binding motifs, suggesting coordinated DNA binding of E2A with these TFs (Fig. 3B). E2A-binding sites identified in this study compared with a previously published enhancer atlas of the developing cortex (Visel et al., 2013) and, together with H3K4Me1, H3K4Me3 and H3K27Ac histone marks (Shen et al., 2012), revealed that E2A predominantly bound enhancer regions (H3K27Ac, H3K4Me1[high], H3K4Me3[low]), which are partially active as indicated by co-occurrence of p300. Promotor regions (H3K27Ac, H3K4Me1[low], H3K4Me3[high]) that are bound by E2A in NSCs show p300 recruitment at later developmental stages (P0), indicating activity at later developmental time points

(Fig. S4A). To determine the biological functions of E2A-bound genes according to enriched gene sets grouped by Gene Ontology (GO) terms, we used GREAT (Genomic Regions Enrichment of Annotations Tool). We found enrichment of the GO categories 'regulation of gliogenesis', 'brain development' and 'stem cell maintenance' (Fig. 3C). Several core genes responsible for the regulation of cortical brain development, including *Foxg1*, *Pax6* and *Sox5* are found within these enriched GO categories, suggesting that E2A serves as a central player in controlling corticogenesis. Currently, E2A target genes in embryonic NSCs during cortical development are unknown. Interestingly, although our ChIP-Seq did not reveal binding of E2A to previously described binding sites in the E-cadherin gene (Pérez-Moreno et al., 2001), we confirmed binding to sites in *Cdkn1a* [which encodes p21(CIP1) protein] (Fig. 3D) (Prabhu et al., 1997). Analysis of E2A occupancy of related CDKI genes in embryonic NSCs revealed several E2A-binding sites in the *Cdkn1b* [encodes p27(KIP1) protein] and *Cdkn1c* [encodes p57(KIP2) protein] loci (Fig. 3E,F). The three sites of E2A occupancy at the *Cdkn1c* locus in embryonic NSCs (Fig. 3F), which we termed 'p57-I' (intron), 'p57-II' (downstream) and 'p57-III' (distal intergenic) correspond to a potentially poised enhancer (H3K4Me1 only, p57-I), an active enhancer (H3K27Ac, H3K4Me1, p57-II) and a *Cdkn1c* promoter (H3K27Ac, H3K4Me3>H3K4Me, p57-III) (Fig. 3F), suggesting that these E2A-binding sites in the *Cdkn1c* locus are putative regulatory elements. Three biological replicates of the ChIP-Seq experiment showed a high degree of overlap between E2A-bound sites and, importantly, all E2A-binding sites within the *Cdkn1c* locus were confirmed (Fig. S4B).

E12 and E47 share binding sites with differential transcriptional outcome

To obtain genome-wide binding patterns of the E12 and E47 splice variant of E2A, we performed ChIP-Seq in E12^{−/−} and E47^{−/−} primary embryonic NSCs. Surprisingly, 67% of the identified E2A peaks were detected in both genotypes and greater than 90% of the reproducible E2A peaks in wild-type cells were also found by E2A in both E12- and E47-deficient primary embryonic NSCs (Fig. 4A). This indicates a high redundancy of E12 and E47 in their ability to recognize E2A enhancer. Motif analysis as well as GO enrichment for the overlapping E2A cistrome in these genotypes confirmed the results obtained in wild type (Fig. 3B,C), pointing out 'somatic stem cell maintenance', 'gliogenesis' and 'neurogenesis' among the most enriched pathways. Surprisingly, whole-genome transcriptome analysis by RNA sequencing (RNA-Seq) revealed astonishing differences in gene expression between E12^{−/−} and E47^{−/−} primary embryonic NSCs when compared with their respective littermate wild-type controls (Fig. 4B). Only 60 genes were identified as commonly differentially expressed in E12^{−/−} and E47^{−/−} cells (Table S1), emphasizing their distinct functions in this tissue. In order to identify the genes directly regulated by E12 and/or E47, we filtered the differentially expressed genes by the occurrence of a close by E2A peak in wild type (Venn diagram in Fig. 3B). 55.3% of the differentially expressed genes in E47^{−/−} cells and 34.6% of the differentially expressed genes in E12^{−/−} embryonic NSCs were predicted to be direct E2A target genes. A closer look at the direct E47 target genes (Table S2) revealed that 181 genes were induced upon loss of E47, whereas only 50 genes were repressed, indicating that E47 acts as a repressor in this context. In contrast, E12 target genes were mostly repressed (85 genes compared with 42 induced genes, Table S3), predicting an activating function of E12 at these loci. Besides the differences observed in the regulatory potential of
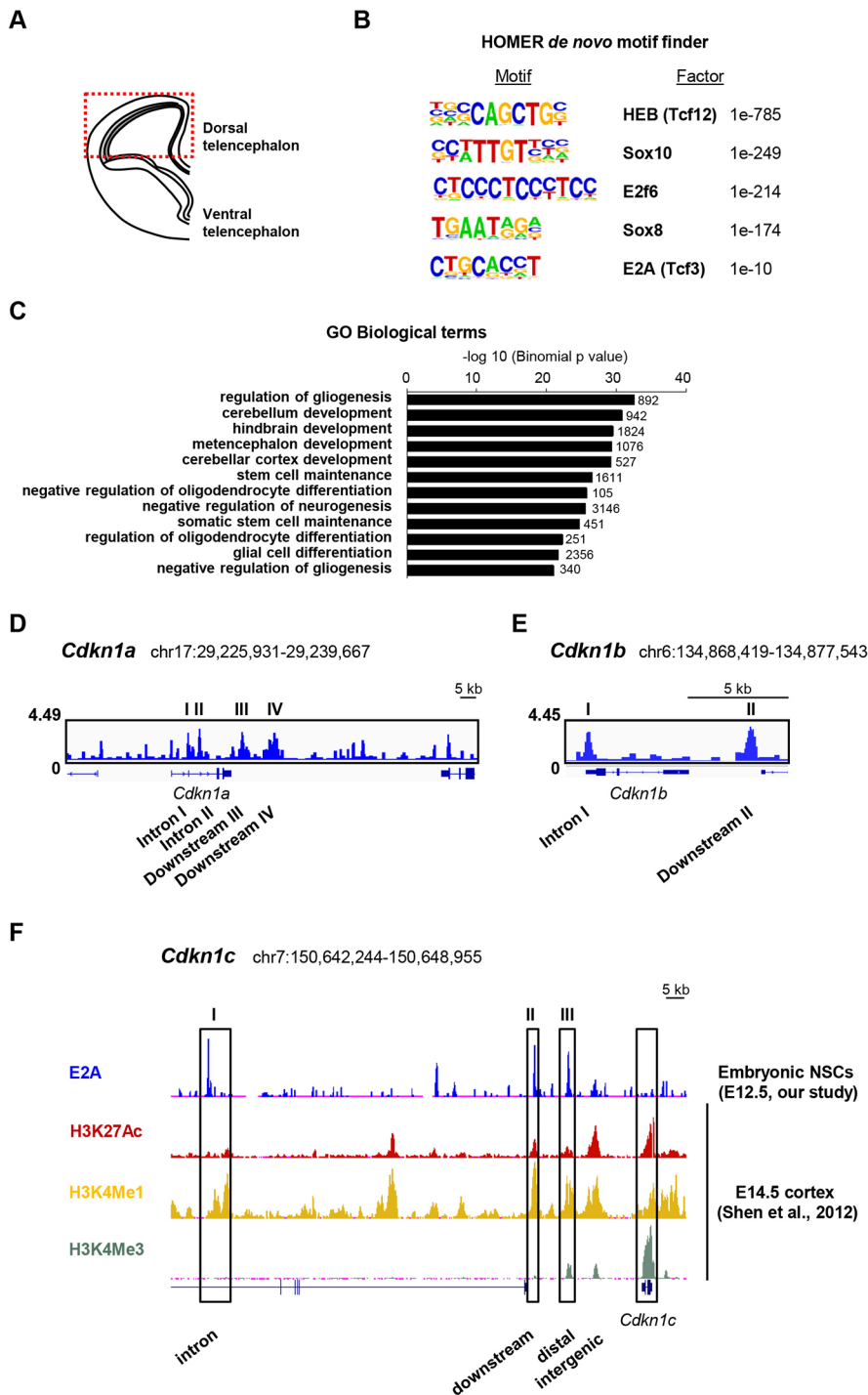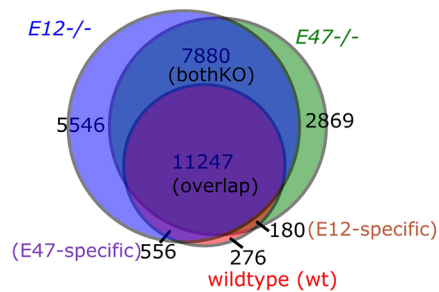
Fig. 3. Identification of E2A-binding sites in embryonic NSC chromatin using ChIP Seq. (A) Scheme of one cortical hemisphere at developmental stage E12.5. The red rectangle indicates the region of embryonic NSCs isolated for ChIP-Seq. (B) Motifs enriched in E2A-bound segments from a *de novo* search using HOMER software. *Cis*-regulatory sequences associated with E2A occupancy in embryonic NSCs were identified by comparison of enriched binding sites with randomly selected genomic DNA sequences. Letter size indicates nucleotide frequency. Log *P* values for the *cis*-regulatory sequences associated bHLH factor HEB (Tcf12), Sox10, E2f6, Sox8 and E2A (*Tcf3*) are indicated on the right. (C) Analysis of enrichment of Gene Ontology (GO) terms by GREAT for biological processes associated with E2A-bound genes. The number of target genes in each category is shown on the right of each bar. (D,E) A representative panel of E2A binding at the *Cdkn1a* locus (D) and *Cdkn1b* locus (E) in embryonic NSC chromatin. (F) A representative panel of E2A occupancy at the *Cdkn1c* locus in embryonic NSC chromatin in comparison with E2A histone marks in the cortex at E14.5 (Shen et al., 2012). Histone marks indicate that p57-I corresponds to a potential poised enhancer (H3K4Me1 only), whereas p57-II and p57-III are active enhancers (H3K27Ac, H3K4Me1). E2A peaks are indicated by roman numbers and peak heights are shown as numbers of sequenced reads.

the two E2A splice isoforms, GO enrichment analysis of the respective target genes revealed distinct functions for E47 and E12 in primary embryonic NSCs (Fig. 4B, right). E47 target genes induce biological processes as 'negative regulation of glia cell differentiation' (e.g. *Hmga2*, *Notch1*, *Dll3* and *Hes5*) and 'negative regulation of nervous system development' (e.g. *Ednrb* and *Lingo1*). E12 target genes on the other hand represent a variety of developmental biological processes (e.g. *Kit*, *Myc* and *Tgfbr2*), including 'axon development' (e.g. *Arhgef3* and *Nfasc*) and 'cell-cell adhesion' (*Sema4d* and *Has2*). To indicate the E2A binding pattern in wild-type, E12$^{-/-}$ and E47$^{-/-}$ embryonic NSCs of one of
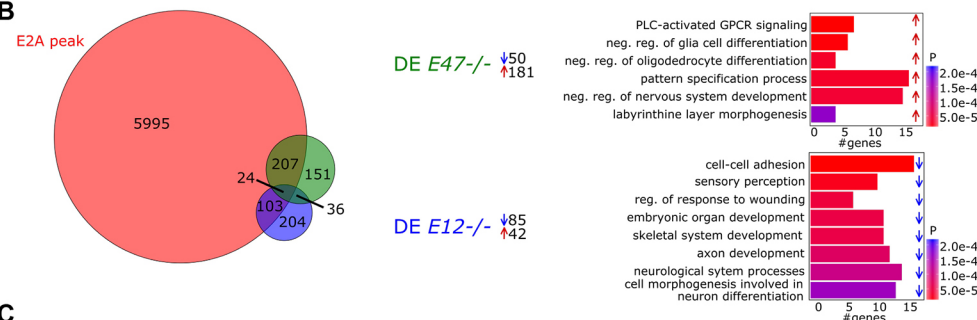
the genes differentially regulated by the E2A splice variants, we choose the *Cdkn1c* gene locus as an example (Fig. 3F, Fig. 4C). In wild-type NSCs, we observed four peaks upstream of the *Cdkn1c* gene locus (black boxes in Fig. 4C below wild-type track). These peaks are bound by E2A in E12$^{-/-}$ as well as in E47$^{-/-}$ embryonic NSCs. The strong signal in the E47$^{-/-}$ NSCs in intron 1 of the *Kcnq1* gene locus on the other hand was not identified as a peak by MACS and seems to be an artefact as many of the reads mapped here have identical start and end positions (PCR artefact, Fig. 4C). From analysis of E2A-binding events in wild-type, E12- and E47-deficient embryonic NSCs, we conclude that E12 and E47 are able
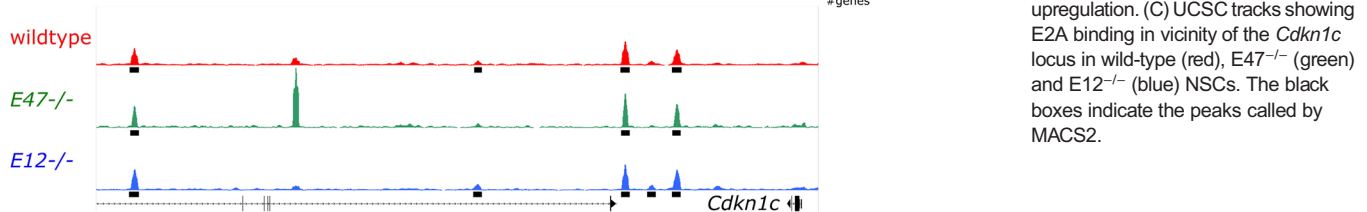
Fig. 4. Overlapping E47 and E12 cistromes with distinct transcriptional outputs. (A) ChIP-Seq analysis of E2A binding in wild-type, E12$^{-/-}$ and E47$^{-/-}$ primary embryonic NSCs. The Venn diagram indicates the proportion of E2A-binding sites overlapping or exclusively identified in wild-type, E12$^{-/-}$ and/or E47$^{-/-}$ NSCs, respectively. The table indicates the identified transcription factor-binding motifs and functional annotation according to the GO_Biological Process for each of the population subsets identified in the Venn diagram. The motifs identified from the overlapping E2A peaks of wild-type, E12$^{-/-}$ and E47$^{-/-}$ were also identified in all other E2A peak subsets and are not indicated repetitively. Overlap indicates common peaks in wild type, E12$^{-/-}$ and E47$^{-/-}$; both KO indicates shared E2A peaks in E12$^{-/-}$ and E47$^{-/-}$ but not wild-type peaks; E47$^{-/-}$indicates E2A peaks 'gained' in E47$^{-/-}$; E12$^{-/-}$ indicates E2A peaks 'gained' in E12$^{-/-}$; E47-specific indicates E2A peaks lost only in E47$^{-/-}$; E12-specific indicates E2A peaks lost only in E12$^{-/-}$. (B) Transcriptome analysis of E12$^{-/-}$ and E47$^{-/-}$ primary embryonic NSCs by RNA-Seq. The Venn diagram indicates the overlap in genes that are differentially expressed (fold change>1.5-fold) in E12$^{-/-}$ (blue) or E47$^{-/-}$ (green) cells compared with their respective wild-type littermate controls and the genes that have an E2A-binding site in their proximity. The bar plots indicate the functional annotation of the differentially expressed genes with a wild-type E2A peak close according to GO_Biological Process. Blue arrows refer to downregulation. Red arrows indicate upregulation. (C) UCSC tracks showing E2A binding in vicinity of the *Cdkn1c* locus in wild-type (red), E47$^{-/-}$ (green) and E12$^{-/-}$ (blue) NSCs. The black boxes indicate the peaks called by MACS2.

to bind the same sites, but differentially affect gene expression by recruitment of either differential interaction partners or co-regulators.

E47 directly regulates p57(KIP2) expression in embryonic NSCs by binding to a distal *Cdkn1c* enhancer

Next, we performed quantitative PCR using E47$^{-/-}$ embryonic NSCs to reveal whether E2A-bound CDKI genes were regulated by E47. Quantitative PCR revealed a halving, albeit not significant reduction of *Cdkn1c* mRNA expression in E47$^{-/-}$ embryonic NSCs compared with wild-type littermate cultures (Fig. S5A left), while *Cdkn1a* and *Cdkn1b* gene expression was not altered (Fig. S5A, middle, right). Immunolabeling for p57(KIP2) at E14.5 revealed a significant decrease in the p57(KIP2) expression in E47$^{-/-}$ embryos compared with wild-type embryos (Fig. 5A,B), while p57(KIP2) was not altered at E12.5 (Fig. S5B,C). In addition, no significant regulation of p57(KIP2) expression was observed in E12$^{-/-}$ embryos compared with wild-type embryos (Fig. S5D,E). To identify putative regulatory elements in the *Cdkn1c* locus that are controlled by E47, we cloned each of the identified E2A-binding regions (p57-I-III, Fig. 3F) upstream of a luciferase gene driven by the minimal *Admlp2* promoter and co-transfected HEK293T cells with these reporters and increasing amounts of E47. We found that E47 increased the activity of the 'p57-I' element in a dose-
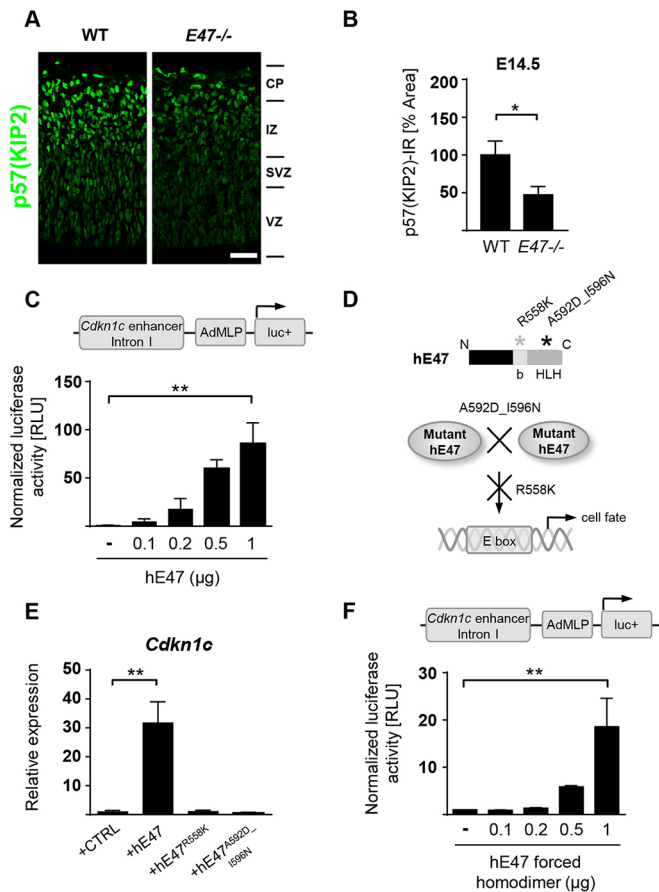
DEVELOPMENT

Fig. 5. E47 directly regulates p57(KIP2) expression in embryonic NSCs.
(A) Immunolabeling for p57(KIP2) (A, green) in sagittal brain sections of E47$^{-/-}$ mice compared with wild-type littermates at E14.5. Scale bar: 40 µm.
(B) Quantification of the p57(KIP2) immunoreactivity (*n*=6 wild-type mice, *n*=8 E47$^{-/-}$ mice). (C) Luciferase reporter assay in HEK293T cells using the indicated *Cdkn1c* luciferase reporter construct (*Cdkn1c* enhancer I termed as intron). Luciferase reporter assay results are of three independent experiments performed in duplicate. (D) Scheme illustrating mutations of the human E47 protein (mutation positions are indicated by asterisks). The hE47^{R558K}-IRES-eGFP plasmid encodes a hE47 mutant, which can dimerize and interact with potential co-factors, but cannot bind to the DNA. The hE47$^{A592D\_I596N}$-IRES-eGFP plasmid encodes a hE47 mutant, which cannot dimerize with other bHLH TFs (Voronova and Baltimore, 1990). (E) Expression of *Cdkn1c* mRNA in embryonic NSCs 24 h after electroporation with the hE47 plasmid in comparison with cells electroporated with mutant hE47^{R558K}-IRES-eGFP and mutant hE47$^{A592D\_I596N}$-IRES-eGFP plasmid or pCAGGs-IRES-eGFP control plasmid determined by quantitative PCR and normalized to *Gapdh*. Quantitative PCR results are of two independent experiments performed in duplicate. (F) Luciferase reporter assay in HEK293T cells using the indicated *Cdkn1c* luciferase reporter construct (*Cdkn1c* enhancer I termed as intron). Luciferase reporter assay results are from three independent experiments performed in duplicate. Data are mean±s.e.m. **$P<0.01$; *$P<0.05$ by Student's *t*-test (B) and one-way ANOVA (C,E,F). RLU, relative light unit.

dependent manner [human E47 (hE47), 86±21.59-fold (±s.e.m.), $P<0.01$; Fig. 5C], whereas E47 did not significantly affect the activities of the 'p57-II' and 'p57-III' regions (Fig. S5F,G). We next analyzed whether dimerization and DNA binding of E47 is required for *Cdkn1c* expression. Therefore, we used either an E47 mutant that cannot form homo- or heterodimers (A592D_I596N) owing to mutations in the HLH region (black asterisk) or an E47 mutant that is able to form dimers but cannot bind DNA (R558K) due to a mutation in the basic region of the protein (gray asterisk) (Fig. 5D).

(Voronova and Baltimore, 1990). Equal expression of the E47 mutants in embryonic NSCs was validated by western blot analysis (Fig. S5H). *Cdkn1c* mRNA expression was significantly increased in cells expressing wild-type hE47 in comparison with control cell cultures electroporated with an empty vector [hE47, 33±7.26-fold (±s.e.m.); $P<0.01$; Fig. 5E]. In accordance with the mRNA expression data of *Cdkn1a* and *Cdkn1b* in E47$^{-/-}$ embryonic NSCs (Fig. S5A, middle, right), hE47 expression in embryonic NSCs did not alter *Cdkn1a* and *Cdkn1b* gene expression (Fig. S5K). To test whether E47 interacts with proneural bHLH factors to regulate *Cdkn1c*, we performed co-immunoprecipitation on lysates from embryonic neural stem cells. E47 did not interact with any tested non-bHLH proteins (Limk) nor with bHLH TFs (NeuroD1, NeuroD2, Math2, Mash1, and Ngn2) in primary NSCs, suggesting a yet unknown interaction partner for E47 or E47 might primarily act as a homodimer (Fig. S5I). Indeed, overexpression of an E47 forced homodimer (E47FD) (Sigvardsson et al., 1997) (Fig. S5J, validation of expression by western blot analysis) increased the activity of the 'p57-I' element in a dose-dependent manner (Fig. 5F).

E47 overexpression regulates NSC differentiation and localization

The E47 regulated CDKI p57(KIP2) has been shown to regulate cellular processes, including proliferation, cell cycle exit and differentiation of embryonic NSCs (Mairet-Coello et al., 2012; Tury et al., 2011, 2012). To determine the role of E47 in these biological processes, we analyzed cortices of E47$^{-/-}$ embryos and control littermates for cell proliferation (Ki67$^+$ cells) and for cell cycle dynamics by analyzing cumulative EdU labeling (2-h intervals) in Ki67$^+$ neuronal precursors. We did not detect any significant differences in cell proliferation and cell cycle length in E47$^{-/-}$ embryos at E14.5 compared with control littermates (Fig. 6A,B) or at E12.5 (Ki67$^+$ neuronal cell and Edu$^+$Ki67$^+$ cells at 2 h after injection, data not shown). In addition, immunostaining for phosphohistone H3 (pH3), an indicator of late G2- and M-phase (Hendzel et al., 1997) revealed no difference in apical and basal divisions in E47$^{-/-}$ embryos at E14.5 compared with control littermates (Fig. 6C,D and data not shown). Accordingly, neither proliferation nor apoptosis of E47$^{-/-}$ embryonic NSCs was altered compared with wild-type cells *in vitro* (Fig. 6E,F; Fig. S6A,B). However, analysis of E47$^{-/-}$ embryonic NSCs revealed a difference in the distribution of the size of neurospheres formed compared with wild-type embryonic NSCs, with increased numbers of bigger neurospheres formed by E47$^{-/-}$ compared with wild-type cells (Fig. S6C). Yet, the total number of single cells within the dissociated neurospheres did not differ between E47$^{-/-}$ and control cells (data not shown), suggesting no difference in proliferation, but possibly differences in single cell size or cell-adhesion properties (Marthiens et al., 2010). To identify whether E47 regulates NSC differentiation, we overexpressed E47 in primary embryonic NSCs, which resulted in a reduced number of cells with neurite outgrowth [hE47, 23.1±6.3% and control, 75.48±6.8% (±s.e.m.); $P<0.01$: Fig. 7A,B] compared with control NSCs (pCAGGs-IRES-eGFP, referred to as CTRL). Furthermore, overexpression of the E47 non-DNA-binding mutant (hE47^{R558K}) showed an increased number of cells with neurite outgrowth compared with wild-type hE47 overexpression (Fig. 7A,B). We next investigated the effect of E47 on neuronal differentiation and localization *in vivo* by *in utero* electroporation of wild-type embryos at E13.5. E47-overexpressing cells (GFP$^+$) showed reduced neurite outgrowth [hE47, 7.45±4.0% and control, 50.22±4.78% (±s.e.m.); $P<0.001$: Fig. 7C,D] and had a
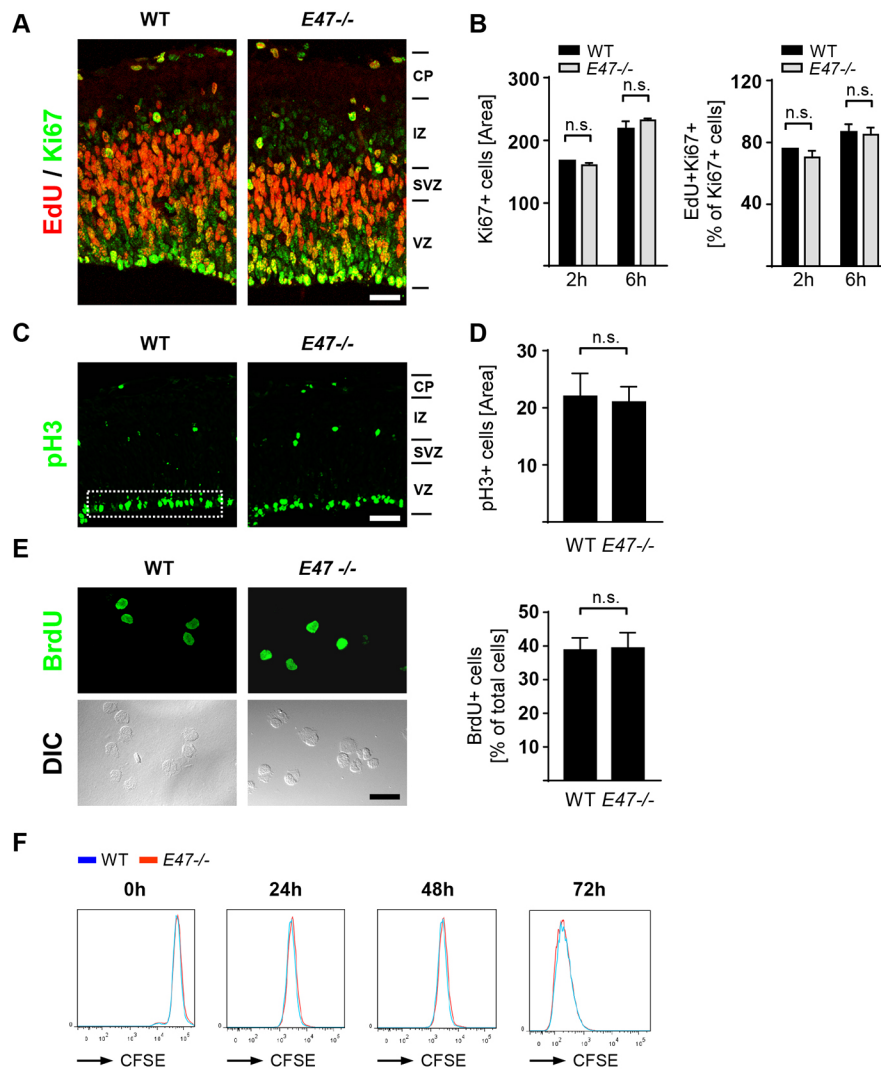
Fig. 6. E47 deficiency does not affect cell cycle length of embryonic NSCs and intermediate precursor cells. (A) Immunolabeling for EdU (red) in combination with Ki67 (green) in the cortex in sagittal brain sections of E47$^{-/-}$ mice and wild-type littermates at E14.5 2 h after EdU injection. Scale bar: 40 µm. (B) Quantification of the number of proliferating precursors (Ki67$^+$) (n=3 wild-type mice, n=4 E47$^{-/-}$ mice) and quantification of the number of proliferating precursors and SVZ precursors in S phase (Ki67$^+$EdU$^+$ per Ki67$^+$) per area of quantification (n=1 wild-type mice, n=3 E47$^{-/-}$ mice, 2 h; n=2 wild-type mice, n=2 E47$^{-/-}$ mice, 6 h). (C) Immunolabeling for phospho-histone H3 (green) in sagittal brain sections of E47$^{-/-}$ mice and wild-type littermates at E14.5. Scale bar: 55 µm. (D) Quantification of the number of phospho-histone H3$^+$ cells (n=5 wild-type mice, n=4 E47$^{-/-}$ mice). (E) Immunolabeling for BrdU of E47$^{-/-}$ and wild-type embryonic NSCs after a 4 h BrdU pulse (left) and quantification of immunolabeled BrdU$^+$ cells (right). Scale bar: 20 µm. BrdU labeling results are from four independent experiments. A minimum of 200 cells per condition were analyzed. (F) Labeling of E47$^{-/-}$ and wild-type embryonic NSCs by CFSE and measurement of CFSE intensity by flow cytometry 0, 24, 48 and 72 h after labeling. CFSE labeling results are from two independent experiments. Data are mean±s.e.m. P-values were calculated using Student's t-test. BrdU, 5-bromo-2′-deoxyuridine; CFSE, carboxyfluorescein succinimidyl ester; DIC, differential interference contrast; EdU, 5-ethynyl-2′-deoxyuridine; CP, cortical plate; IZ, intermediate zone; SVZ, subventricular zone; VZ, ventricular zone; pH3, phospho-histone H3.

more apical position in the cortex, mainly in the IZ [hE47, 0.22± 0.22, and control, 1.00±0.14 (±s.e.m.); P<0.05: Fig. 7C,E]. E47 overexpressing cells did not differentiate into Tbr1$^+$ deep layer neurons, as did controls (Fig. 7F). Further characterization of the E47 overexpression cells revealed that these cells are NeuroD1$^+$ intermediate zone precursor cells (Fig. 7G, Fig. S7). The E47-regulated CDKI p57(KIP2) has been shown to regulate cellular processes, including differentiation of embryonic NSCs (Mairet-Coello et al., 2012; Tury et al., 2011, 2012). To investigate, whether E47 regulates NSC differentiation via regulation of p57(KIP2), we overexpressed p57(KIP2) in primary embryonic E47$^{-/-}$ NSCs. E47$^{-/-}$ NSCs already had a tendency to have an increased number of cells with neurite outgrowth when compared with wild-type NSCs (Fig. 7H,I). Importantly, p57(KIP2) overexpression in primary embryonic E47$^{-/-}$ NSCs resulted in a reduced number of cells with neurite outgrowth {mouse p57(KIP2) [mp57 (KIP2)], 23.5±9.5%; control, 43.7±10.4% (±s.e.m.); P<0.01: Fig. 7H,I}. In line with these results, *in vivo* overexpression of E47 resulted in increased p57(KIP2) expression, while p57 (KIP2) protein could not be detected in sections of embryos electroporated with control plasmid (Fig. 7J,K). Together, these results suggest that, in embryonic NSCs, increased abundance of E47 leads to impaired neuronal differentiation and localization by upregulation of the CDKI p57(KIP2).

DISCUSSION
The *Tcf3* locus (E2A) encodes two highly related proteins, E12 and E47, that arise through mutually exclusive splicing of two alternative exons and differ only in their DNA-binding region (Murre et al., 1989). Recently, distinct roles for E12 and E47 in B cell specification have been demonstrated (Beck et al., 2009). Our results suggest that the E2A splice variant E47 is required for proper neuronal differentiation and layer-specific localization, whereas the E2A splice variant E12 is likely dispensable for early corticogenesis. E2A regulates cell type specification and differentiation programs, including neurogenesis during embryonic development, by dimerization with tissue-specific class II HLH proteins (Gradwohl et al., 1996; Lee, 1997; Wang and Baker, 2015). Thus, an important unresolved issue is whether E2A functions independently of neurogenic class II bHLH TFs. *Ngn2;Mash1* double-mutant embryos have a severe disruption of the cortical cytoarchitecture (Nieto et al., 2001) and *Ngn* mutant embryos show a specification defect of neural precursor cells, resulting in abnormal localization of early-born deep-layer neurons during dorsal telencephalon development (Casarosa et al., 1999; Fode et al., 2000; Li et al., 2012; Nieto et al., 2001; Schuurmans et al., 2004). In contrast, our data revealed a specific role for E47 in regulating the population size of Tbr1$^+$ and Satb2$^+$ projection neurons, while neuronal regional identity and the overall cortical
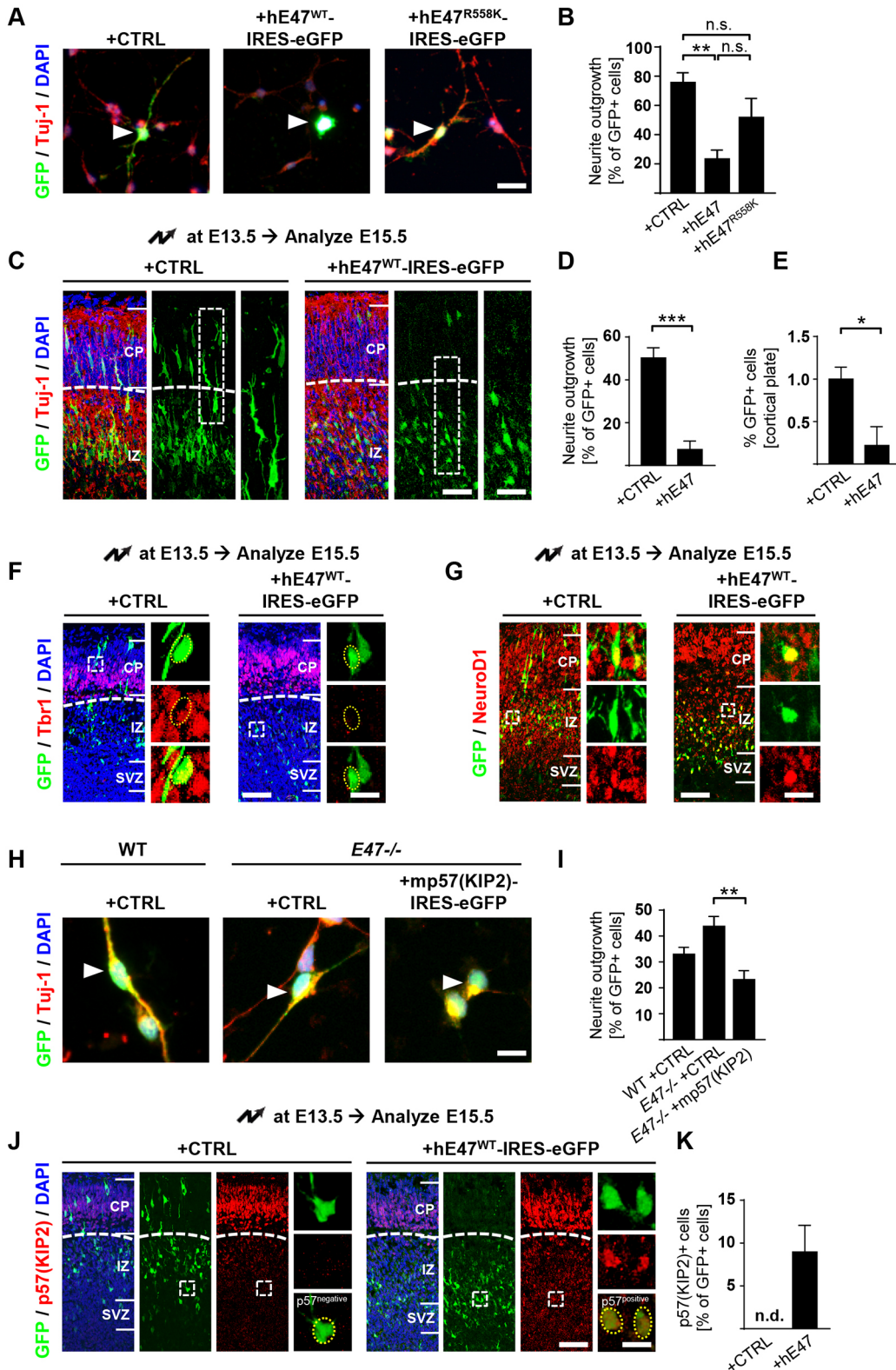
Fig. 7. See next page for legend.

cytoarchitecture was not affected. Thus, with regard to heterodimerization with class II bHLH TFs, Mash1 and Ngn are not strictly dependent on E47. The interaction with Mash1 as a key TF in ventral telencephalon development is unlikely to mediate E47-regulated differentiation of projection neurons with dorsal

telencephalon identity (Fode et al., 2000), as it was shown that the specification of these cells is Ngn dependent. Furthermore, E47 might function independently of Ngn during early neurogenesis, as Ngn1/Ngn2 are required to specify the cortical, glutamatergic and laminar characteristics of early-born neurons, while simultaneously

Fig. 7. E47 regulates NSC differentiation via p57(KIP2). (A) Immunolabeling for Tuj-1 (red, neurons) and GFP (green, electroporated cells) 2 days after electroporation of primary NSCs with wild-type hE47 plasmid (hE47^{WT}-IRES-eGFP) in comparison with mutant (hE47^{R558K}-IRES-eGFP) and control plasmid (CTRL, pCAGGs-IRES-eGFP) cultured under differentiation conditions on laminin. Nuclei are stained with DAPI (blue). Arrowhead indicates a representative electroporated cell per condition. Scale bar: 20 µm. (B) Quantification of the number of electroporated GFP$^+$ cells showing neurite outgrowth in embryonic NSCs overexpressing wild-type hE47, hE47^{R558K} or control plasmid. Results are from four different experiments. A minimum of 130 cells per condition was analyzed. (C) *In utero* electroporation of wild-type mice at E13.5 with either pCAGGs-IRES-eGFP or hE47^{WT}-IRES-eGFP. Immunolabeling was performed for Tuj-1 (red, neurons) and GFP (green, electroporated cells) in sagittal brain sections at E15.5. Enlargements of regions outlined show inhibition of neurite outgrowth and mislocalization of cells expressing hE47^{WT}-IRES-eGFP (right) compared with control (pCAGGs-IRES-eGFP) (left). Nuclei are stained with DAPI (blue). Scale bars: 40 µm (left); 20 µm (right). (D,E) Quantification of the number of GFP$^+$ cells showing neurite outgrowth (D) or located in the cortical plate (CP) (E) in sections of E15.5 embryos after *in utero* electroporation (D: n=3 CTRL, n=4 hE47; E: n=6 CTRL, n=5 hE47). (F,G) Immunolabeling for Tbr1 (F, red, deep layer neurons), NeuroD1 (G, red, intermediate zone cells) and GFP (green, electroporated cells) in sagittal brain sections at E15.5. Enlargements of regions outlined show E47-overexpressing cells that are GFP$^+$Tbr1$^-$ cells (right) compared with control cells that are GFP$^+$Tbr1$^+$ cells (left) (F), and NeuroD1$^+$GFP$^+$ cells in the intermediate zone (G). Nuclei are stained with DAPI (blue). (H) Immunolabeling for Tuj-1 (red, neurons) and GFP (green, electroporated cells) 1 day after electroporation of primary E47$^{-/-}$ NSCs with mp57(KIP2) plasmid [mp57(KIP2)-IRES-eGFP] in comparison with control plasmid (pCAGGs-IRES-eGFP) cultured under differentiation conditions on laminin. Nuclei are stained with DAPI (blue). Arrowheads depict a representative electroporated cell per condition. Scale bar: 10 µm. (I) Quantification of the number of electroporated GFP$^+$ cells showing neurite outgrowth in embryonic E47$^{-/-}$ NSCs overexpressing mp57(KIP2) or control plasmid. Results are from four different experiments. A minimum of 100 cells per condition was analyzed. (J) *In utero* electroporation of wild-type mice at E13.5 with either pCAGGs-IRES-eGFP or hE47^{WT}-IRES-eGFP. Immunolabeling for p57(KIP2) (red) and GFP (green) was performed in sagittal sections of the cortex at E15.5. Enlargements of regions indicated by rectangles show GFP$^+$p57(KIP2)$^+$ cells (right, yellow circle) and GFP$^+$p57(KIP2)$^-$ cells (left, yellow circle). Scale bars: 65 µm (left); 10 µm (right). Nuclei are stained with DAPI (blue). (K) Quantification of the number of p57(KIP2)$^+$GFP$^+$ cells in sections of E15.5 embryos after *in utero* electroporation (n=3 pCAGGs-IRES-eGFP, n=4 hE47-IRES-eGFP). Data are mean±s.e.m. ***P<0.001; **P<0.01; *P<0.05 using one-way ANOVA (B,I) and Student's t-test (D,E,K). Dotted line indicates the border between the cortical plate (CP) and IZ/SVZ area (C,F,G,J). CP, cortical plate; IZ, intermediate zone; SVZ, subventricular zone.

repressing an alternative subcortical, GABAergic neuronal phenotype (Schuurmans et al., 2004). In contrast, E47 regulated the differentiation of Tbr1-positive deep layer and Satb2-positive upper layer projection neurons at E14.5, whereas E47 depletion did not result in an alternative subcortical, GABAergic neuronal phenotype. At this point a role for E2A as a heterodimerization partner of neurogenic class II bHLH TFs during early dorsal telencephalon development cannot be excluded; in E47-deficient embryos, other E proteins, such as E12, E2-2 and HEB might compensate for the loss of E47 at specific developmental time points. Our data revealed overlapping expression of E47 and E12 in NSCs and our ChIP-Seq identified a big overlap for E12- and E47-specific binding sites in embryonic NSCs, supporting possible functional redundancy among individual E proteins at different developmental time points. However, protein stability in differentiating cells (Fig. 1G), post-translational modifications (Teachenor et al., 2012), heterodimerization partner or co-factor recruitment (Gow et al., 2014) at specific developmental time points in specific cell populations further adds complexity to the specific functions of individual E proteins in cortical development. Indeed,

our RNA-Seq analysis revealed that the splice-isoform E47 acts mainly as a transcriptional repressor in NSCs, while E12 target genes are reduced in E12$^{-/-}$ primary embryonic NSCs, pointing towards a distinct transcriptional regulatory mechanism exploited by each of the two E2A splice isoforms.

As E47 overexpression *in vitro* and *in vivo* showed neuronal differentiation defects resulting in impaired neurite outgrowth, another potential interaction partner could be NeuroD due to its function in neuritogenesis (Bayam et al., 2015; Ince-Dunn et al., 2006). Indeed, the comparison of our E2A ChIP-Seq data with a genome-wide NeuroD2 DNA-binding analysis (Bayam et al., 2015) revealed largely overlapping NeuroD2 binding around E2A peaks, including the 'p57-I' intronic enhancer of *Cdkn1c*. We detected no interaction of E47 with putative binding partners, including NeuroD1/2 in primary embryonic NSCs, suggesting a potential role for E47 homodimers. Indeed, our luciferase assays revealed that E47 homodimers regulate *Cdkn1c* expression independently of pro-neurogenic class II bHLH heterodimerization partner. Future studies will show whether E47 might act as a homodimer or in combination with an as yet unknown TF to regulate the differentiation of Tbr1$^+$ and Satb2$^+$ projection neurons.

E2A proteins play key roles in controlling gene expression during development of many tissues, such as in B and T cell development (Murre, 2005). Yet, no E2A target genes are known for cortex development. Target genes have been described for the potential E2A interaction partners Mash1, Ngn1/2 and NeuroD. A genome-wide study for Mash1 characterized target genes during ventral telencephalon development (Castro et al., 2011), whereas a genome-wide study for NeuroD2 (genes with functions in layer-specific differentiation and in axonal pathfinding) and target genes for Ngn2 [*Etv1*, *HuD* (*Elav4*) and *Rnd2*] have been described for dorsal telencephalon development (Bayam et al., 2015; Bronicki et al., 2012; Heng et al., 2008; Kovach et al., 2013). The E2A-activated transcriptional program described here provides evidence that E2A indeed induces many TFs and other regulators of specification and differentiation of embryonic NSCs, e.g. Foxg1 (Martynoga et al., 2005), Pax6 (Warren et al., 1999) and Sox5 (Kwan et al., 2008), suggesting that E2A is actively involved in the balanced coordination of the neurogenic program in cortical development.

E proteins are not functionally equivalent as they function independently, resulting in E protein-specific phenotypes (Beck et al., 2009) and as they regulate specific target genes in different immune cell lineages (Lin et al., 2010; Sanda et al., 2012); however, no E2A splice variant target genes are known for cortex development. Our genome-wide DNA-binding analysis of E12 and E47 revealed similar binding patterns of both splice variants. E2A peaks 'lost' in splice variant-deficient mice suggest occupancy of E47 and E12 splice variant homo- or heterodimerzation at E2A binding sites. We speculate at this point that the two splice variants of E2A are able to compensate for each other's loss at the level of target site DNA binding. In contrast, RNA-Seq analysis of target gene regulation revealed a unique role for E12 and E47 in regulating transcription of certain genes. Specifically, our data suggest that E47 might mainly work by repressing genes, while E12 seems to work as a transcriptional activator of genes in embryonic neural stem cells. This is in line with a role for E47 as a transcriptional repressor of a subset of astrocyte-specific genes in adult NSC differentiation (Bohrer et al., 2015). E2A binding to the *Cdkn1c* gene locus was detected in E12- and E47-deficient embryonic NSCs, albeit expression of *Cdkn1c* was altered only upon deletion of E47 and remained stable in the absence of E12. Thus, splice

variant-specific transcriptional gene regulation detected in our study were in line with phenotypic differences observed in E12$^{-/-}$ and E47$^{-/-}$ mice, suggesting that E12 and E47 might have similar DNA-binding capabilities, but splice-variant specific DNA binding may result in distinct regulatory mechanisms (e.g. by recruitment of different co-regulators) that differentially affect gene expression. This may affect gene expression of various other genes and not only of *Cdkn1c* during cortical development.

A function for E2A as cell cycle regulator has been proposed and E2A-binding sites in CDKI genes have been described outside the nervous system (Pagliuca et al., 2000; Prabhu et al., 1997). Although our study identified E2A-binding sites in the *Cdkn1a*, *Cdkn1b* and *Cdkn1c* loci, E47 overexpression, knockout experiments and luciferase reporter assays revealed that, among those, only the *Cdkn1c* gene is a regulated E47 target gene during cortical development. A previous study indicated that potential *Cdkn1c* enhancers are located between +35 and +225 kb from the *Cdkn1c* transcription start site (John et al., 2001) and a putative muscle-specific enhancer was recently identified to be localized to a conserved 686 bp fragment lying ∼+59 kb from *Cdkn1c* that is controlled by the bHLH TF MyoD (Zalc et al., 2014). This muscle-specific enhancer element corresponds to one site of E12 and E47 occupancy in embryonic NSCs ['p57-I' (intron)] identified by our ChIP-Seq data and was classified as a poised enhancer in mESCs by analyzing histone marks (Shen et al., 2012). Furthermore, E47 was able to activate transcription from this enhancer, suggesting that it not only acts as an enhancer in muscle cell differentiation, but might be developmentally regulated in several tissues. However, here it is not activated by MyoD, but presumably by E47 heterodimers or homodimers, and functions as a regulatory element in neuronal localization and differentiation during corticogenesis.

Cell cycle and differentiation in the developing forebrain are intimately connected (Salomoni and Calegari, 2010; Tury et al., 2011). Blocking the cell cycle induces neural-progenitor differentiation and migration from the VZ to upper cortical regions (Calegari and Huttner, 2003; Lange et al., 2009). p57(KIP2) as a member of CDKIs is able to block the progression of the cell cycle in embryonic (Furutachi et al., 2015) and adult NSCs (Furutachi et al., 2013) by predominantly binding and inhibiting cyclin/CDK complexes of the G1 phase. Surprisingly, we did not observe functions of E47 for the regulation of cell proliferation and cell cycle length during early cortical development at E14.5. In addition to the well-characterized function of p57(KIP2) in regulating cell cycle progression, it also has been shown to control NSC migration and differentiation (Mairet-Coello et al., 2012; Tury et al., 2011, 2012). *Cdkn1c*-deficient mice reveal an increase in layer V to VI neurons (Mairet-Coello et al., 2012). Despite E2A and p57(KIP2) expression in SVZ/IZ cells during early- and mid-corticogenesis (Fig. 1C, Fig. S1C) (Tury et al., 2012; data not shown), E47 might regulate p57(KIP2) expression in a defined time window to control Tbr1$^+$ and Satb2$^+$ cortical projection neuron differentiation at mid-neurogenesis. Indeed, our data revealed that E47 regulated p57(KIP2) at a specific developmental time point during corticogenesis.

Interestingly, p57(KIP2) regulates cell differentiation and migration via direct interaction with several bHLH TFs, such as Mash1, NeuroD1/2 and Nex/Math2, and actin cytoskeleton-modifying enzymes, such as Limk1/2 (Joseph et al., 2009; Vlachos and Joseph, 2009). NeuroD2 was recently identified as an early-onset neuronal transcript with protein expression detected in newborn apical VZ neurons (Telley et al., 2016) and p57(KIP2) expression was shown to colocalize with NeuroD1 in postmitotic cells in the IZ (Tury et al., 2012). Our data showed that the overexpression of p57(KIP2) in E47$^{-/-}$ NSCs inhibited neurite outgrowth, similar to E47 overexpression in wild-type NSCs, suggesting a linear relationship between E47 and p57(KIP2) expression in the differentiating projection neurons during cortical development. Future studies will determine whether E47 dynamically controls p57(KIP2) expression, which then might direct neurogenesis of Tbr1$^+$ and Satb2$^+$ projection neurons by abundant p57(KIP2) interacting with NeuroD.

We identified a specific role for E47 in regulating Tbr1$^+$ and Satb2$^+$ projection neurons via p57(KIP2) during cortical development, while Ctip2$^+$ projection neurons were not affected. The sequence and pace of neuronal differentiation processes of different neuronal subtypes is instructed by sequential transcriptional waves (Telley et al., 2016). The birthdates of cortical neurons are known to correspond to their particular cortical layer position (Smart and Smart, 1982), as is the case for layer VI Tbr1$^+$ and layer V Ctip2$^+$ subcortical layer projection neurons. Birthdating experiments revealed that even Ctip2$^+$ neurons in layer V are earlier born than Satb2$^+$ callosal projection neurons in layer V (Hatanaka et al., 2016). Therefore, E47 might control distinct temporally gated genetic targets and networks in different cell populations, such as the identified p57(KIP2) target in this study, that affect distinct neuronal subpopulation localization and differentiation. Misbalanced neurogenesis is associated with autism-like features (Fang et al., 2014) and, more specifically, altered Tbr1 expression and function is associated with autism (Deriziotis et al., 2014; Huang et al., 2014; Notwell et al., 2016). As E47 is regulating Tbr1$^+$ and Satb2$^+$ projection neuron cell numbers during cortical development, it would be very interesting to investigate whether dysregulated E47 is linked to Tbr1-related autism spectrum disorders.

Overall, we identified a specific role for E47 in regulating Tbr1$^+$ and Satb2$^+$ projection neurons via p57(KIP2) during cortical development. Beside its function in brain development, p57(KIP2) has been implicated in adult NSC quiescence and neurogenesis (Furutachi et al., 2013, 2015), cancer (Borriello et al., 2011; Guo et al., 2010), and human disorders (Duquesnes et al., 2016; John et al., 2001; Zhang et al., 1997). The *Cdkn1c* locus has been implicated in the Beckwith-Wiedemann syndrome, a growth-regulation disorder characterized by tissue overgrowth and predisposition to tumors (Zhang et al., 1997), and mutations in different predicted enhancers have been suggested to contribute to the formation of the disease (Eggermann et al., 2014). Aberrant p57(KIP2) expression might be evoked through misbalanced E47 protein activity or mutations in the E47-responsive enhancer. Thus, the consequent targeting of E47 activity and the direct regulation of p57(KIP2) by the distant E47-regulated 'p57-I' enhancer identified in this study might offer novel therapeutic opportunities for p57(KIP2)-associated diseases.

MATERIALS AND METHODS
Animals
C57BL/6J mice (Jackson Laboratory), C57BL/6J-inbred mice deficient for the E2A splice variant E12 (E12$^{-/-}$) or E47 (E47$^{-/-}$) (Beck et al., 2009), *Eomes*^{GFP} mice (Arnold et al., 2009) and *Hes5::CreE*^{RT}*2Rosa26-CAG:: eGFP*$^{fl/+}$ (Rolando et al., 2016) were used. Mouse brains were isolated from embryos of various developmental stages as indicated. The morning of vaginal plug was considered as being embryonic day 0.5 (E0.5). All animal experiments were approved by the Federal Ministry for Nature, Environment and Consumer Protection of the state of Baden-Württemberg and were performed in accordance to the respective national, federal and institutional regulations.

Immunohistochemistry

Embryonic mouse brains were dissected and fixed in 4% paraformaldehyde (PFA) in phosphate-buffered saline (PBS) at 4°C overnight. After cryoprotection by immersion in 30% sucrose solution, brain samples were embedded in OCT (Tissue-Tek). Immunohistochemistry on sagittal brain cryostat sections was performed as described previously (Schachtrup et al., 2015). Details of immunohistochemistry and antibodies used are described in the supplementary Materials and Methods.

In situ hybridization (ISH)

Nonradioactive ISH was performed on cryosections of wild-type mice using a *Tcf3*-specific probe. For details of ISH, see the supplementary Materials and Methods.

Embryonic NSC culture

Embryonic NSCs from E14.5 embryos were isolated and cultured as described (Bohrer et al., 2015; Reynolds and Weiss, 1992). For differentiation conditions, embryonic NSCs were plated on laminin (1 µg/ml; Sigma-Aldrich) in NSC medium without rhFGF-2 and rhEGF. For neurosphere size measurements, 200 dissociated embryonic NSCs per well were cultured in a 96-well plate (BD) in NSC medium with growth factors for 7 days. The diameter of at least 200 neurospheres was measured as recently described (Nam and Benezra, 2009). For proliferation assays, dissociated embryonic NSCs were cultured in NSC proliferation medium for 24 h, treated with BrdU (1:100, Invitrogen) for 4 h, followed by cytospin and immunolabeling. Additionally, proliferation was tested by labeling NSCs with carboxyfluorescein diacetate succinimidyl ester (CFSE) by incubating 2×10^6 cells/ml in PBS containing 1 µM CFSE for 10 min at 37°C. Embryonic NSCs were harvested at different time points, resuspended in FACS buffer (PBS+1% BSA) containing propidium iodide (1 µM), and immediately analyzed by flow cytometry. Data were collected with the LSRII flow cytometer (BD Biosciences) and analyzed with FlowJo software (Tree Star). For E47 overexpression experiments, wild-type embryonic NSCs were transfected by electroporation using the Mouse Neural Stem Cell Nucleofector Kit (Lonza) following the manufacturer's instructions with hE47^{WT}-IRES-eGFP, hE47^{R558K}-IRES-eGFP or pCAGGs-IRES-eGFP control plasmids (1.5 µg). For p57(KIP2) overexpression experiments, wild-type or E47$^{-/-}$ embryonic NSCs were transfected by electroporation using the Mouse Neural Stem Cell Nucleofector Kit (Lonza) following manufacturer's instructions with mp57(KIP2)-IRES-eGFP or pCAGGs-IRES-eGFP control plasmids (1.5 µg).

Immunocytochemistry

Immunocytochemistry was performed as described previously (Schachtrup et al., 2015) and further details are described in the supplementary Materials and Methods.

Neurite outgrowth assay

Neurite outgrowth assays were performed as previously described using electroporated embryonic NSCs (Schachtrup et al., 2010). Details of the neurite outgrowth assay and analysis are described in the supplementary Materials and Methods.

RNA isolation and quantitative PCR

RNA was isolated from primary embryonic NSCs and quantitative PCR was performed as described previously (Schachtrup et al., 2010). Primer pairs used are described in the supplementary Materials and Methods.

RNA sequencing (RNA-Seq)

RNA isolation from primary embryonic E12$^{-/-}$, and E47$^{-/-}$ NSCs and respective littermate controls at 14.5 was performed as described previously (Schachtrup et al., 2010). The quality of the RNA was verified using an Agilent 2100 Bioanalyzer with RNA 6000Nano Reagents (Agilent Technologies). Library preparation and rRNA depletion was performed using the TruSeq Stranded mRNA Library Prep Kit (Illumina) starting with 500 ng RNA as input for each sample. Libraries were sequenced on the Illumina HiSeq4000. Sequencing quality was assessed with FastQC (http://

www.bioinformatics.babraham.ac.uk/projects/fastqc/). The reads were mapped to the mouse genome mm9 (Ensembl build 37.67) and reads per gene counted using STAR (Dobin, 2013) with the following settings: –outFilterType BySJout –outFilterMultimapNmax 20 –alignSJoverhangMin 8 – alignSJDBoverhangMin 1 –outFilterMismatchNmax 999 –outFilter MismatchNoverLmax 0.04 –alignIntronMin 20 –alignIntronMax 1000000 –alignMatesGapMax 100000 –quantMode GeneCounts. The gene annotation information was obtained from Ensembl (build 37.67). Gene count normalization and differential expression analysis was performed using DESeq2 (Love et al., 2014). For gene annotation, biomaRt was used (Durinck et al., 2009). Functional enrichment according to gene ontology was carried out using clusterProfiler (Yu et al., 2012).

Chromatin immunoprecipitation sequencing (ChIP-Seq)

Chromatin immunoprecipitation (ChIP) assays were performed as described (Beck et al., 2009). Details on the ChIP procedure and antibodies used are described in the supplementary Materials and Methods. Purified chromatin was analyzed by high-throughput DNA sequencing on an Illumina HiSeq 3000 as described previously (Uhlenhaut et al., 2013). Reads were aligned to the mouse mm9 reference genome using BWA-MEM version 0.7.13 (Li, 2013 preprint) and PCR duplicates removed using Picard Tools version 1.119 (http://picard.sourceforge.net/). For the visualization of the tracks, mapped reads were converted to bedGraph using the HOMER software suite version 4.8.3 (Heinz et al., 2010) and visualized in the UCSC genome browser (Kent et al., 2002). Peaks were called using MACS2 version 2.1.0 (Zhang et al., 2008) and Gene Ontology analysis performed with GREAT (McLean et al., 2010). Motif discovery and read distribution analysis around E2A peaks was conducted with HOMER. The binding profiles of NeuroD2 (GSE67539) (Bayam et al., 2015) and p300 (GSE42881) (Visel et al., 2013), as well as the H3K4Me1, H3K4Me3, H3K27Ac modification profile (GSE29218) (Shen et al., 2012), were obtained from GEO (Edgar et al., 2002).

Luciferase reporter transactivation assays

The luciferase reporter construct was generated by cloning three putative *Cdkn1c* regulatory elements defined by E2A binding, termed *Cdkn1c* intron (chr7: 150,587,437-150,587,805), *Cdkn1c* downstream (chr7: 150,614,405-150,614,750) and *Cdkn1c* distal intergenic (chr7: 150,623,726-150,624,250), into the pGL3-Admlp2 plasmid (Sayegh et al., 2003). Each fragment was isolated by PCR amplification using C57BL/6J mouse genomic DNA. Details of the luciferase assay procedure and primers used for cloning of reporter constructs are described in the supplementary Materials and Methods.

Co-immunoprecipitation

For endogenous co-immunoprecipitation, cell lysates of primary embryonic NSC cultures were incubated with rabbit anti-mouse E2A antibody (5 µg; sc-349X, Santa Cruz Biotechnology) bound to A-agarose beads for 4 h at 4°C. Details of co-immunoprecipitation are provided in the supplementary Materials and Methods.

Immunoblots

For detection of E47 and E12 expression in wild-type, E47$^{-/-}$ and E12$^{-/-}$ embryonic NSCs, primary cells cultured in proliferation medium were harvested. To detect E12 and E47 expression in wild-type NSCs under proliferating and differentiating conditions, primary cells were cultured in NSC proliferation medium and in NSC differentiation medium for various times. For expression analysis of E47 and E12 in primary NSCs and human E47 and GFP in electroporated embryonic NSCs from wild-type mice, protein extracts were sampled and separated by electrophoresis on 8% and 10% SDS-PAGE gels as described previously (Schachtrup et al., 2010). Antibodies used are described in the supplementary Materials and Methods.

EdU labeling regime

To analyze relative cell cycle length of embryonic NSCs in the cortex, EdU (30 mg/kg body weight, Thermo Fisher) was injected intraperitoneally into

DEVELOPMENT

pregnant dams at E12.5 or E14.5. Cumulative EdU labeling of $E47^{-/-}$ and wild-type littermate mouse embryos (C57BL/6 background) at E14.5 was performed by repeated intraperitoneal injections (2 h intervals) into pregnant mice as previously described (Calegari et al., 2005). Relative changes in cell cycle length were assessed by EdU/Ki67 dual immunolabeling of embryonic mouse brain sections collected 2 h and 6 h after EdU injection. The total number of $EdU^+/Ki67^+$ cells was counted within the VZ and SVZ (Mairet-Coello et al., 2012).

In utero electroporation
Plasmid DNA for electroporation was generated under endotoxin-free conditions using the EndoFree Plasmid Maxi Kit (Qiagen). *In utero* electroporation was performed as previously described (Knuckles et al., 2012). DNA constructs were injected into the lateral ventricles of each embryo at E13.5 of pregnancy in C57BL/6J mice and the embryos were allowed to develop until E15.5 before isolation. Details of the *in utero* electroporation procedure are described in the supplementary Materials and Methods.

Microscopy and imaging analysis
Images were collected using either an Axioplan 2 Imaging epifluorescence microscope, an AxioImager.M2 epifluorescence microscope, a TCS SP8 confocal laser scanning microscope or a Leica DM LED Fluo inverted microscope. Details on microscopy, image processing and quantification are described in the supplementary Materials and Methods.

Statistical analysis
Data are shown as mean±s.e.m. Differences between groups were analyzed by one-way ANOVA followed by Bonferroni's post-test for multiple comparisons. Differences between isolated pairs were examined using Student's *t*-test.

References
Arnold, S. J., Sugnaseelan, J., Groszer, M., Srinivas, S. and Robertson, E. J. (2009). Generation and analysis of a mouse line harboring GFP in the Eomes/Tbr2 locus. *Genesis* **47**, 775-781.

Bayam, E., Sahin, G. S., Guzelsoy, G., Guner, G., Kabakcioglu, A. and Ince-Dunn, G. (2015). Genome-wide target analysis of NEUROD2 provides new insights into regulation of cortical projection neuron migration and differentiation. *BMC Genomics* **16**, 681.

Beck, K., Peak, M. M., Ota, T., Nemazee, D. and Murre, C. (2009). Distinct roles for E12 and E47 in B cell specification and the sequential rearrangement of immunoglobulin light chain loci. *J. Exp. Med.* **206**, 2271-2284.

Bedogni, F., Hodge, R. D., Elsen, G. E., Nelson, B. R., Daza, R. A. M., Beyer, R. P., Bammler, T. K., Rubenstein, J. L. R. and Hevner, R. F. (2010). Tbr1 regulates regional and laminar identity of postmitotic neurons in developing neocortex. *Proc. Natl. Acad. Sci. USA* **107**, 13129-13134.

Bohrer, C., Pfurr, S., Mammadzada, K., Schildge, S., Plappert, L., Hils, M., Pous, L., Rauch, K. S., Dumit, V. I., Pfeifer, D. et al. (2015). The balance of Id3 and E47 determines neural stem/precursor cell differentiation into astrocytes. *EMBO J.* **34**, 2804-2819.

Borriello, A., Caldarelli, I., Bencivenga, D., Criscuolo, M., Cucciolla, V., Tramontano, A., Oliva, A., Perrotta, S. and Della Ragione, F. (2011). p57Kip2 and cancer: time for a critical appraisal. *Mol. Cancer Res.* **9**, 1269-1284.

Bronicki, L. M., Belanger, G. and Jasmin, B. J. (2012). Characterization of multiple exon 1 variants in mammalian HuD mRNA and neuron-specific transcriptional control via neurogenin 2. *J. Neurosci.* **32**, 11164-11175.

Calegari, F. and Huttner, W. B. (2003). An inhibition of cyclin-dependent kinases that lengthens, but does not arrest, neuroepithelial cell cycle induces premature neurogenesis. *J. Cell Sci.* **116**, 4947-4955.

Calegari, F., Haubensak, W., Haffner, C. and Huttner, W. B. (2005). Selective lengthening of the cell cycle in the neurogenic subpopulation of neural progenitor cells during mouse brain development. *J. Neurosci.* **25**, 6533-6538.

Casarosa, S., Fode, C. and Guillemot, F. (1999). Mash1 regulates neurogenesis in the ventral telencephalon. *Development* **126**, 525-534.

Castro, D. S., Martynoga, B., Parras, C., Ramesh, V., Pacary, E., Johnston, C., Drechsel, D., Lebel-Potter, M., Garcia, L. G., Hunt, C. et al. (2011). A novel function of the proneural factor Ascl1 in progenitor proliferation identified by genome-wide characterization of its targets. *Genes Dev.* **25**, 930-945.

Deriziotis, P., O'Roak, B. J., Graham, S. A., Estruch, S. B., Dimitropoulou, D., Bernier, R. A., Gerdts, J., Shendure, J., Eichler, E. E. and Fisher, S. E. (2014). De novo TBR1 mutations in sporadic autism disrupt protein functions. *Nat. Commun.* **5**, 4954.

Duquesnes, N., Callot, C., Jeannot, P., Daburon, V., Nakayama, K. I., Manenti, S., Davy, A. and Besson, A. (2016). p57^Kip2 knock-in mouse reveals CDK-independent contribution in the development of Beckwith-Wiedemann syndrome. *J. Pathol.* **239**, 250-261.

Dobin, A. (2013) STAR: ultrafast universal RNA-seq aligner. *Bioinformatics* **29**, 15-21.

Durinck, S., Spellman, P. T., Birney, E. and Huber, W. (2009). Mapping identifiers for the integration of genomic datasets with the R/Bioconductor package biomaRt. *Nat. Protoc.* **4**, 1184-1191.

Edgar, R., Domrachev, M. and Lash, A. E. (2002). Gene Expression Omnibus: NCBI gene expression and hybridization array data repository. *Nucleic Acids Res.* **30**, 207-210.

Eggermann, T., Binder, G., Brioude, F., Maher, E. R., Lapunzina, P., Cubellis, M. V., Bergadá, I., Prawitt, D. and Begemann, M. (2014). CDKN1C mutations: two sides of the same coin. *Trends Mol. Med.* **20**, 614-622.

Fang, W.-Q., Chen, W.-W., Jiang, L., Liu, K., Yung, W.-H., Fu, A. K. Y. and Ip, N. Y. (2014). Overproduction of upper-layer neurons in the neocortex leads to autism-like features in mice. *Cell Rep.* **9**, 1635-1643.

Fode, C., Ma, Q., Casarosa, S., Ang, S. L., Anderson, D. J. and Guillemot, F. (2000). A role for neural determination genes in specifying the dorsoventral identity of telencephalic neurons. *Genes Dev.* **14**, 67-80.

Furutachi, S., Matsumoto, A., Nakayama, K. I. and Gotoh, Y. (2013). p57 controls adult neural stem cell quiescence and modulates the pace of lifelong neurogenesis. *EMBO J.* **32**, 970-981.

Furutachi, S., Miya, H., Watanabe, T., Kawai, H., Yamasaki, N., Harada, Y., Imayoshi, I., Nelson, M., Nakayama, K. I., Hirabayashi, Y. et al. (2015). Slowly dividing neural progenitors are an embryonic origin of adult neural stem cells. *Nat. Neurosci.* **18**, 657-665.

Gow, C.-H., Guo, C., Wang, D., Hu, Q. and Zhang, J. (2014). Differential involvement of E2A-corepressor interactions in distinct leukemogenic pathways. *Nucleic Acids Res.* **42**, 137-152.

Gradwohl, G., Fode, C. and Guillemot, F. (1996). Restricted expression of a novel murine atonal-related bHLH protein in undifferentiated neural precursors. *Dev. Biol.* **180**, 227-241.

Guo, H., Tian, T., Nan, K. and Wang, W. (2010). p57: a multifunctional protein in cancer (review). *Int. J. Oncol.* **36**, 1321-1329.

Hatanaka, Y., Namikawa, T., Yamauchi, K. and Kawaguchi, Y. (2016). Cortical divergent projections in mice originate from two sequentially generated, distinct populations of excitatory cortical neurons with different initial axonal outgrowth characteristics. *Cereb. Cortex* **26**, 2257-2270.

Heinz, S., Benner, C., Spann, N., Bertolino, E., Lin, Y. C., Laslo, P., Cheng, J. X., Murre, C., Singh, H. and Glass, C. K. (2010). Simple combinations of lineage-determining transcription factors prime cis-regulatory elements required for macrophage and B cell identities. *Mol. Cell* **38**, 576-589.

Hendzel, M. J., Wei, Y., Mancini, M. A., Van Hooser, A., Ranalli, T., Brinkley, B. R., Bazett-Jones, D. P. and Allis, C. D. (1997). Mitosis-specific phosphorylation of histone H3 initiates primarily within pericentromeric heterochromatin during G2 and spreads in an ordered fashion coincident with mitotic chromosome condensation. Chromosoma 106, 348-360.

Heng, J. I.-T., Nguyen, L., Castro, D. S., Zimmer, C., Wildner, H., Armant, O., Skowronska-Krawczyk, D., Bedogni, F., Matter, J.-M., Hevner, R. et al. (2008). Neurogenin 2 controls cortical neuron migration through regulation of Rnd2. Nature 455, 114-118.

Huang, T.-N., Chuang, H.-C., Chou, W.-H., Chen, C.-Y., Wang, H.-F., Chou, S.-J. and Hsueh, Y.-P. (2014). Tbr1 haploinsufficiency impairs amygdalar axonal projections and results in cognitive abnormality. Nat. Neurosci. 17, 240-247.

Imayoshi, I. and Kageyama, R. (2014). bHLH factors in self-renewal, multipotency, and fate choice of neural progenitor cells. Neuron 82, 9-23.

Ince-Dunn, G., Hall, B. J., Hu, S.-C., Ripley, B., Huganir, R. L., Olson, J. M., Tapscott, S. J. and Ghosh, A. (2006). Regulation of thalamocortical patterning and synaptic maturation by NeuroD2. Neuron 49, 683-695.

John, R. M., Ainscough, J. F., Barton, S. C. and Surani, M. A. (2001). Distant cis-elements regulate imprinted expression of the mouse p57Kip2(Cdkn1c)gene: implications for the human disorder, Beckwith–Wiedemann syndrome. Hum. Mol. Genet. 10, 1601-1609.

Joseph, B., Andersson, E. R., Vlachos, P., Södersten, E., Liu, L., Teixeira, A. I. and Hermanson, O. (2009). p57Kip2 is a repressor of Mash1 activity and neuronal differentiation in neural stem cells. Cell Death Differ. 16, 1256-1265.

Kent, W. J., Sugnet, C. W., Furey, T. S., Roskin, K. M., Pringle, T. H., Zahler, A. M. and Haussler, D. (2002). The human genome browser at UCSC. Genome Res. 12, 996-1006.

Knuckles, P., Vogt, M. A., Lugert, S., Milo, M., Chong, M. M. W., Hautbergue, G. M., Wilson, S. A., Littman, D. R. and Taylor, V. (2012). Drosha regulates neurogenesis by controlling neurogenin 2 expression independent of microRNAs. Nat. Neurosci. 15, 962-969.

Kovach, C., Dixit, R., Li, S., Mattar, P., Wilkinson, G., Elsen, G. E., Kurrasch, D. M., Hevner, R. F. and Schuurmans, C. (2013). Neurog2 simultaneously activates and represses alternative gene expression programs in the developing neocortex. Cereb. Cortex 23, 1884-1900.

Kwan, K. Y., Lam, M. M. S., Krsnik, Z., Kawasawa, Y. I., Lefebvre, V. and Sestan, N. (2008). SOX5 postmitotically regulates migration, postmigratory differentiation, and projections of subplate and deep-layer neocortical neurons. Proc. Natl. Acad. Sci. USA 105, 16021-16026.

Kwan, K. Y., Sestan, N. and Anton, E. S. (2012). Transcriptional co-regulation of neuronal migration and laminar identity in the neocortex. Development 139, 1535-1546.

Lange, C., Huttner, W. B. and Calegari, F. (2009). Cdk4/cyclinD1 overexpression in neural stem cells shortens G1, delays neurogenesis, and promotes the generation and expansion of basal progenitors. Cell Stem Cell 5, 320-331.

Lee, J. E. (1997). Basic helix-loop-helix genes in neural development. Curr. Opin. Neurobiol. 7, 13-20.

Li, H. (2013). Aligning sequence reads, clone sequences and assembly contigs with BWA-MEM. arXiv:1303.3997.

Li, S., Mattar, P., Zinyk, D., Singh, K., Chaturvedi, C.-P., Kovach, C., Dixit, R., Kurrasch, D. M., Ma, Y.-C., Chan, J. A. et al. (2012). GSK3 temporally regulates neurogenin 2 proneural activity in the neocortex. J. Neurosci. 32, 7791-7805.

Lin, Y. C., Jhunjhunwala, S., Benner, C., Heinz, S., Welinder, E., Mansson, R., Sigvardsson, M., Hagman, J., Espinoza, C. A., Dutkowski, J. et al. (2010). A global network of transcription factors, involving E2A, EBF1 and Foxo1, that orchestrates B cell fate. Nat. Immunol. 11, 635-643.

Love, M. I., Huber, W. and Anders, S. (2014). Moderated estimation of fold change and dispersion for RNA-seq data with DESeq2. Genome Biol. 15, 550.

Mairet-Coello, G., Tury, A., Van Buskirk, E., Robinson, K., Genestine, M. and DiCicco-Bloom, E. (2012). p57KIP2 regulates radial glia and intermediate precursor cell cycle dynamics and lower layer neurogenesis in developing cerebral cortex. Development 139, 475-487.

Marthiens, V., Kazanis, I., Moss, L., Long, K. and Ffrench-Constant, C. (2010). Adhesion molecules in the stem cell niche–more than just staying in shape? J. Cell Sci. 123, 1613-1622.

Martynoga, B., Morrison, H., Price, D. J. and Mason, J. O. (2005). Foxg1 is required for specification of ventral telencephalon and region-specific regulation of dorsal telencephalic precursor proliferation and apoptosis. Dev. Biol. 283, 113-127.

McLean, C. Y., Bristor, D., Hiller, M., Clarke, S. L., Schaar, B. T., Lowe, C. B., Wenger, A. M. and Bejerano, G. (2010). GREAT improves functional interpretation of cis-regulatory regions. Nat. Biotechnol. 28, 495-501.

Molyneaux, B. J., Arlotta, P., Menezes, J. R. L. and Macklis, J. D. (2007). Neuronal subtype specification in the cerebral cortex. Nat. Rev. Neurosci. 8, 427-437.

Molyneaux, B. J., Goff, L. A., Brettler, A. C., Chen, H.-H., Brown, J. R., Hrvatin, S., Rinn, J. L. and Arlotta, P. (2015). DeCoN: genome-wide analysis of in vivo transcriptional dynamics during pyramidal neuron fate selection in neocortex. Neuron 85, 275-288.

Murre, C. (2005). Helix-loop-helix proteins and lymphocyte development. Nat. Immunol. 6, 1079-1086.

Murre, C., McCaw, P. S. and Baltimore, D. (1989). A new DNA binding and dimerization motif in immunoglobulin enhancer binding, daughterless, MyoD, and myc proteins. Cell 56, 777-783.

Murre, C., Bain, G., van Dijk, M. A., Engel, I., Furnari, B. A., Massari, M. E., Matthews, J. R., Quong, M. W., Rivera, R. R. and Stuiver, M. H. (1994). Structure and function of helix-loop-helix proteins. Biochim. Biophys. Acta 1218, 129-135.

Nam, H. S. and Benezra, R. (2009). High levels of Id1 expression define B1 type adult neural stem cells. Cell Stem Cell 5, 515-526.

Nieto, M., Schuurmans, C., Britz, O. and Guillemot, F. (2001). Neural bHLH genes control the neuronal versus glial fate decision in cortical progenitors. Neuron 29, 401-413.

Notwell, J. H., Heavner, W. E., Darbandi, S. F., Katzman, S., McKenna, W. L., Ortiz-Londono, C. F., Tastad, D., Eckler, M. J., Rubenstein, J. L. R., McConnell, S. K. et al. (2016). TBR1 regulates autism risk genes in the developing neocortex. Genome Res. 26, 1013-1022.

Pagliuca, A., Gallo, P., De Luca, P. and Lania, L. (2000). Class A helix-loop-helix proteins are positive regulators of several cyclin-dependent kinase inhibitors' promoter activity and negatively affect cell growth. Cancer Res. 60, 1376-1382.

Pérez-Moreno, M. A., Locascio, A., Rodrigo, I., Dhondt, G., Portillo, F., Nieto, M. A. and Cano, A. (2001). A new role for E12/E47 in the repression of E-cadherin expression and epithelial-mesenchymal transitions. J. Biol. Chem. 276, 27424-27431.

Pinto, L. and Gotz, M. (2007). Radial glial cell heterogeneity–the source of diverse progeny in the CNS. Prog. Neurobiol. 83, 2-23.

Prabhu, S., Ignatova, A., Park, S. T. and Sun, X. H. (1997). Regulation of the expression of cyclin-dependent kinase inhibitor p21 by E2A and Id proteins. Mol. Cell. Biol. 17, 5888-5896.

Ravanpay, A. C. and Olson, J. M. (2008). E protein dosage influences brain development more than family member identity. J. Neurosci. Res. 86, 1472-1481.

Reynolds, B. A. and Weiss, S. (1992). Generation of neurons and astrocytes from isolated cells of the adult mammalian central nervous system. Science 255, 1707-1710.

Roberts, V. J., Steenbergen, R. and Murre, C. (1993). Localization of E2A mRNA expression in developing and adult rat tissues. Proc. Natl. Acad. Sci. USA 90, 7583-7587.

Rolando, C., Erni, A., Grison, A., Beattie, R., Engler, A., Gokhale, P. J., Milo, M., Wegleiter, T., Jessberger, S. and Taylor, V. (2016). Multipotency of adult hippocampal NSCs in vivo is restricted by Drosha/NFIB. Cell Stem Cell 19, 653-662.

Ross, S. E., Greenberg, M. E. and Stiles, C. D. (2003). Basic helix-loop-helix factors in cortical development. Neuron 39, 13-25.

Rothschild, G., Zhao, X., Iavarone, A. and Lasorella, A. (2006). E Proteins and Id2 converge on p57Kip2 to regulate cell cycle in neural cells. Mol. Cell. Biol. 26, 4351-4361.

Salomoni, P. and Calegari, F. (2010). Cell cycle control of mammalian neural stem cells: putting a speed limit on G1. Trends Cell Biol. 20, 233-243.

Sanda, T., Lawton, L. N., Barrasa, M. I., Fan, Z. P., Kohlhammer, H., Gutierrez, A., Ma, W., Tatarek, J., Ahn, Y., Kelliher, M. A. et al. (2012). Core transcriptional regulatory circuit controlled by the TAL1 complex in human T cell acute lymphoblastic leukemia. Cancer Cell 22, 209-221.

Sayegh, C. E., Quong, M. W., Agata, Y. and Murre, C. (2003). E-proteins directly regulate expression of activation-induced deaminase in mature B cells. Nat. Immunol. 4, 586-593.

Schachtrup, C., Ryu, J. K., Helmrick, M. J., Vagena, E., Galanakis, D. K., Degen, J. L., Margolis, R. U. and Akassoglou, K. (2010). Fibrinogen triggers astrocyte scar formation by promoting the availability of active TGF-beta after vascular damage. J. Neurosci. 30, 5843-5854.

Schachtrup, C., Ryu, J. K., Mammadzada, K., Khan, A. S., Carlton, P. M., Perez, A., Christian, F., Le Moan, N., Vagena, E., Baeza-Raja, B. et al. (2015). Nuclear pore complex remodeling by p75(NTR) cleavage controls TGF-beta signaling and astrocyte functions. Nat. Neurosci. 18, 1077-1080.

Schuurmans, C., Armant, O., Nieto, M., Stenman, J. M., Britz, O., Klenin, N., Brown, C., Langevin, L.-M., Seibt, J., Tang, H. et al. (2004). Sequential phases of cortical specification involve Neurogenin-dependent and -independent pathways. EMBO J. 23, 2892-2902.

Shen, C. P. and Kadesch, T. (1995). B-cell-specific DNA binding by an E47 homodimer. Mol. Cell. Biol. 15, 4518-4524.

Shen, Y., Yue, F., McCleary, D. F., Ye, Z., Edsall, L., Kuan, S., Wagner, U., Dixon, J., Lee, L., Lobanenkov, V. V. et al. (2012). A map of the cis-regulatory sequences in the mouse genome. Nature 488, 116-120.

Sigvardsson, M., O'Riordan, M. and Grosschedl, R. (1997). EBF and E47 collaborate to induce expression of the endogenous immunoglobulin surrogate light chain genes. Immunity 7, 25-36.

Smart, I. H. and Smart, M. (1982). Growth patterns in the lateral wall of the mouse telencephalon: I. Autoradiographic studies of the histogenesis of the isocortex and adjacent areas. J. Anat. 134, 273-298.

DEVELOPMENT

Teachenor, R., Beck, K., Wright, L. Y. T., Shen, Z., Briggs, S. P. and Murre, C. (2012). Biochemical and phosphoproteomic analysis of the helix-loop-helix protein E47. *Mol. Cell. Biol.* **32**, 1671-1682.

Telley, L., Govindan, S., Prados, J., Stevant, I., Nef, S., Dermitzakis, E., Dayer, A. and Jabaudon, D. (2016). Sequential transcriptional waves direct the differentiation of newborn neurons in the mouse neocortex. *Science* **351**, 1443-1446.

Tury, A., Mairet-Coello, G. and DiCicco-Bloom, E. (2011). The cyclin-dependent kinase inhibitor p57Kip2 regulates cell cycle exit, differentiation, and migration of embryonic cerebral cortical precursors. *Cereb. Cortex* **21**, 1840-1856.

Tury, A., Mairet-Coello, G. and DiCicco-Bloom, E. (2012). The multiple roles of the cyclin-dependent kinase inhibitory protein p57^{KIP2} in cerebral cortical neurogenesis. *Dev. Neurobiol.* **72**, 821-842.

Uhlenhaut, N. H., Barish, G. D., Yu, R. T., Downes, M., Karunasiri, M., Liddle, C., Schwalie, P., Hübner, N. and Evans, R. M. (2013). Insights into negative regulation by the glucocorticoid receptor from genome-wide profiling of inflammatory cistromes. *Mol. Cell* **49**, 158-171.

Vetter, M. (2001). A turn of the helix: preventing the glial fate. *Neuron* **29**, 559-562.

Visel, A., Taher, L., Girgis, H., May, D., Golonzhka, O., Hoch, R. V., McKinsey, G. L., Pattabiraman, K., Silberberg, S. N., Blow, M. J. et al. (2013). A high-resolution enhancer atlas of the developing telencephalon. *Cell* **152**, 895-908.

Vlachos, P. and Joseph, B. (2009). The Cdk inhibitor p57^{Kip2} controls LIM-kinase 1 activity and regulates actin cytoskeleton dynamics. *Oncogene* **28**, 4175-4188.

Voronova, A. and Baltimore, D. (1990). Mutations that disrupt DNA binding and dimer formation in the E47 helix-loop-helix protein map to distinct domains. *Proc. Natl. Acad. Sci. USA* **87**, 4722-4726.

Wang, L.-H. and Baker, N. E. (2015). E proteins and ID proteins: helix-loop-helix partners in development and disease. *Dev. Cell* **35**, 269-280.

Warren, N., Caric, D., Pratt, T., Clausen, J. A., Asavaritikrai, P., Mason, J. O., Hill, R. E. and Price, D. J. (1999). The transcription factor, Pax6, is required for cell proliferation and differentiation in the developing cerebral cortex. *Cereb. Cortex* **9**, 627-635.

Yu, G., Wang, L.-G., Han, Y. and He, Q.-Y. (2012). clusterProfiler: an R package for comparing biological themes among gene clusters. *OMICS* **16**, 284-287.

Zalc, A., Hayashi, S., Auradé, F., Bröhl, D., Chang, T., Mademtzoglou, D., Mourikis, P., Yao, Z., Cao, Y., Birchmeier, C. et al. (2014). Antagonistic regulation of p57^{kip2} by Hes/Hey downstream of Notch signaling and muscle regulatory factors regulates skeletal muscle growth arrest. *Development* **141**, 2780-2790.

Zhang, P., Liégeois, N. J., Wong, C., Finegold, M., Hou, H., Thompson, J. C., Silverman, A., Harper, J. W., DePinho, R. A. and Elledge, S. J. (1997). Altered cell differentiation and proliferation in mice lacking p57KIP2 indicates a role in Beckwith-Wiedemann syndrome. *Nature* **387**, 151-158.

Zhang, Y., Liu, T., Meyer, C. A., Eeckhoute, J., Johnson, D. S., Bernstein, B. E., Nusbaum, C., Myers, R. M., Brown, M., Li, W. et al. (2008). Model-based analysis of ChIP-Seq (MACS). *Genome Biol.* **9**, R137.

DEVELOPMENT